Seaforth, Loch Seaforth

Bath Medicine Dispersion Modelling Report

███

███████████████████████████████████████

CAR/L/1009963

June 2021

› ██████████

OFFICE
████████████████████████████
████████████

POSTAL
████████████████████████
████████████

PHONE
████████████

FAX
–

MAIL
████████████████████

WEB
████████████████

CONTENTS

Bath Medicine Dispersion Modelling at Loch Seaforth

List of Figures

List of Tables

EXECUTIVE SUMMARY

Dispersion model simulations have been performed to assess whether bath treatments at **Seaforth** salmon farm will comply with pertinent environmental quality standards. Realistic treatment regimes, with 2 pen treatments a day for two days, at both 3-hourly and 4-hourly intervals, and 1 pen treatment for one day, were simulated. Each pen required 1.103 kg of azamethiphos (the active ingredient in Salmosan, Salmosan Vet and Azure) for treatment, resulting in a daily release of up to 2.206 kg and a total discharge over 3 days of 5.515 kg. Simulations were performed separately for neap and spring tides, and the sensitivity of the results to key model parameters was tested.

The model results confirmed that the treatment scenario proposed, with a daily release of no more than 2.206 kg, should comfortably comply with the EQS. The peak concentration during the baseline simulation after 120 hours (72 hours after the final treatment) was less than 0.1 µg/L, the maximum allowable concentration, and the area where concentrations exceeded the EQS of 0.04 µg/L was substantially less than the allowable 0.5 km^2. Results are summarised in Table 1.

Table 1. Summary of Results

SITE DETAILS		
Site Name:	Seaforth	
Site location:	Loch Seaforth	
Peak biomass (T):	2110	
PEN DETAILS		
Number of pens:	5	
Pen dimensions:	160m Circumference	
Working Depth (m):	16	
Pen group configuration:	2 x 2 + 1, 90m matrix	
HYDROGRAPHIC SUMMARY	**ID347**	**ID348**
Surface Currents — Mean Speed (m/s)	0.059	0.052
Residual Speed (m/s)	0.036	0.025
Residual Direction (°G)	351	330
Tidal Amplitude Parallel (m/s)	0.085	0.079
Tidal Amplitude Normal (m/s)	0.022	0.027
Major Axis (°G)	350	325
BATH TREATMENTS		
Recommended consent mass – 3-hr Azamethiphos (g)	1103	
Recommended consent mass – 24-hr Azamethiphos (g)	2206	

The site at Seaforth is managed together with the neighbouring site at Noster. Cumulative modelling of simultaneous treatments at the two sites demonstrated that environmental quality standards were still comfortably met.

A third site in Loch Seaforth with consent to discharge azamethiphos is located at Trilleachan Mor. Cumulative modelling of contemporaneous treatments at all three sites, with a maximum of three treatments in total per day, successfully met the MAC and EQS conditions at both spring and neap tides.

The requested 24-hour mass is substantially larger than the amount predicted by the standard bath model, BathAuto, but the latter is known to be highly conservative, because it does not account for horizontal shearing and dispersion of medicine patches due to spatially-varying current fields, processes which are known to significantly influence dispersion over times scales greater than a few hours (e.g. Okubo, 1971; Edwards, 2015), as illustrated in Figure 10.

1   INTRODUCTION

This report has been prepared by Mowi Scotland Ltd. to meet the requirements of the Scottish Environment Protection Agency (SEPA) for an application to use topical sealice veterinary medicines at the **Seaforth** marine salmon farm in **Loch Seaforth** (Figure **1**). The report presents results from coupled hydrodynamic and particle tracking modelling to describe the dispersion of bath treatments to determine EQS-compliant quantities for the current site biomass and equipment. The modelling procedure follows as far as possible guidance presented by SEPA in June 2019 (SEPA, 2019).
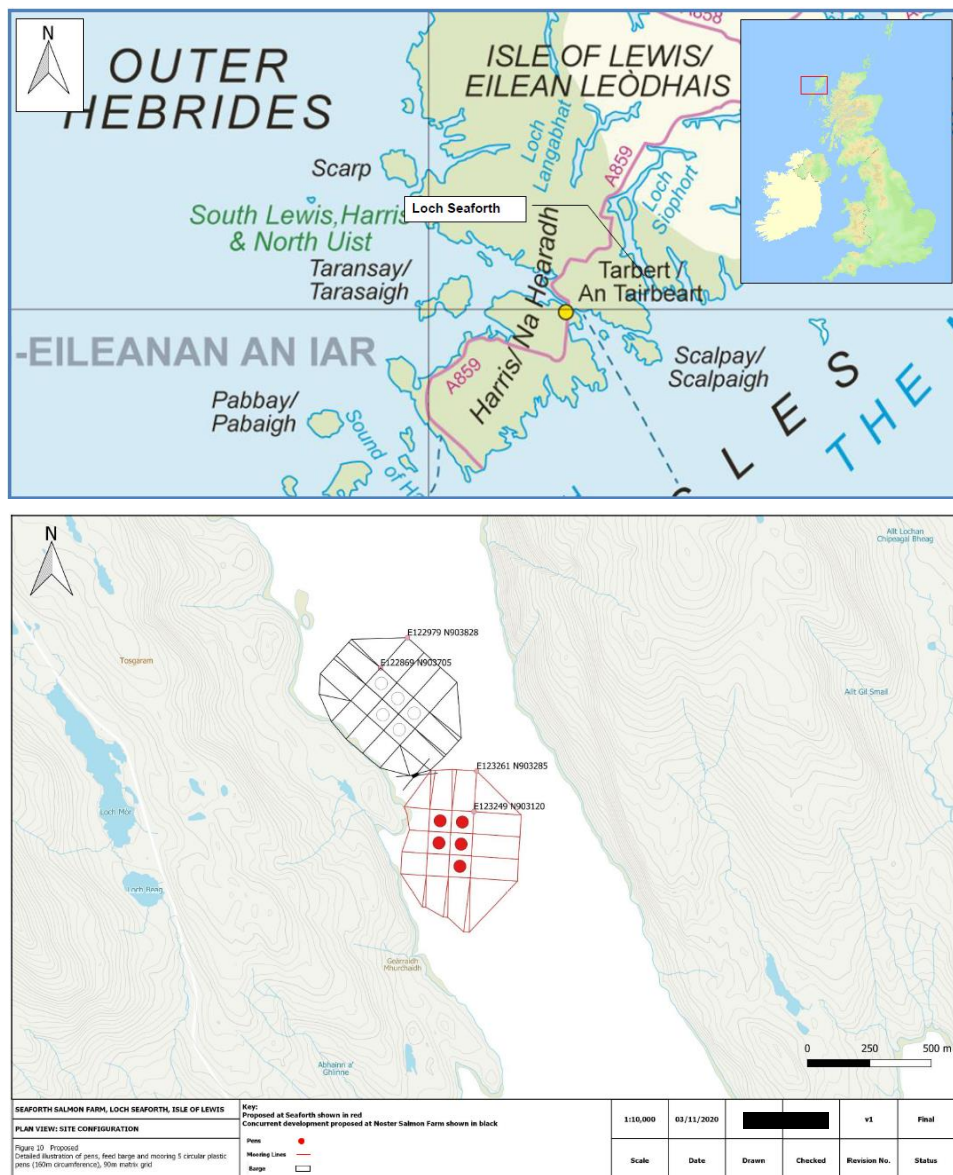
Figure 1. Location of Loch Seaforth (top) and the location of the 160m pens at Seaforth (●). The pens at the Noster site are also shown (○).

1.1   Site Details

The site is situated in the southern part of Loch Seaforth (
Figure **1**). Details of the site are provided in Table 2. The receiving water is defined as a sea loch.

Table 2. Project Information

SITE DETAILS		
Site Name:		Seaforth
Site location:		Loch Seaforth
Peak biomass (T):		2,110
Proposed feed load (T/yr):		5,391
Proposed treatment use:		Azamethiphos
PEN DETAILS		
Group location:		NB23140297
Number of pens:		5
Pen dimensions:		160m circumference
Grid matrix (m)		90
Working Depth (m):		20
Pen group configuration:		2 x 2 + 1
Pen group orientation (°G):		183
Pen group distance to shore (km):		170
Water depth at site (m):		~50
HYDROGRAPHIC DATA		
	ID347	**ID348**
Current meter position:	123097E 903757N	123399E 903120N
Depth at deployment position (m):	67.6	106
Surface bin centre height above bed (m):	50.7	88.7
Middle bin centre height above bed (m):	34.7	72.7
Bottom bin centre height above bed (m):	4.7	4.7
Duration of record (days):	73	73
Start of record:	25th June 2020	25th June 2020
End of record:	6th September 2020	6th September 2020
Current meter averaging interval (min):	20	20
Magnetic correction to grid North:	-3.66	-3.65

2   METHODS

2.1   Model Selection

The modelling approach adopted a coupled hydrodynamic and particle tracking method, whereby water currents in the region, modelled using a calibrated hydrodynamic model, advected particles representing the topical medicine around the model domain. Turbulent eddy diffusion was modelled using a random walk method. Outputs from the modelling were derived to assess the dispersion of the medicine following treatments against statutory Environmental Quality Standards. The modelling approach is described in full in Annex A, and is only summarised here.

For the hydrodynamics, the FVCOM model was used. FVCOM (Finite Volume Community Ocean Model) is a prognostic, unstructured-grid, finite-volume, free-surface, 3-D primitive equation coastal ocean circulation model developed by the University of Massachusetts School of Marine Science and the Woods Hole Oceanographic Institute (Chen et al., 2003). The model consists of momentum, continuity, temperature, salinity and density equations and is closed physically and mathematically using turbulence closure submodels. The horizontal grid is comprised of unstructured triangular cells and the irregular bottom is presented using generalized terrain-following coordinates. The General Ocean Turbulent Model (GOTM) developed by Burchard's research group in Germany (Burchard, 2002) has been added to FVCOM to provide optional vertical turbulent closure schemes. FVCOM is solved numerically by a second-order accurate discrete flux calculation in the integral form of the governing equations over an unstructured triangular grid. This approach combines the best features of finite-element methods (grid flexibility) and finite-difference methods (numerical efficiency and code simplicity) and provides a much better numerical representation of both local and global momentum, mass, salt, heat, and tracer conservation. The ability of FVCOM to accurately solve scalar conservation equations in addition to the topological flexibility provided by unstructured meshes and the simplicity of the coding structure has make FVCOM ideally suited for many coastal and interdisciplinary scientific applications.

The mathematical equations are discretized on an unstructured grid of triangular elements which permits greater resolution of complex coastlines, such as typically found in Scotland. Therefore greater spatial resolution in near-shore areas can be achieved without excessive computational demand. Further details of the FVCOM model and simulations are given in Annex A.

For the particle tracking component, Mowi's in-house model unptrack (Gillibrand, 2021; Annex B) was used. The model used the hydrodynamic flow fields from the FVCOM model simulations. This model has been used previously to simulate sea lice dispersal (Gillibrand & Willis, 2007), the development of a harmful algal bloom (Gillibrand et al., 2016a) and the dispersion of cypermethrin from a fish farm (Willis et al., 2005). The approach for veterinary medicines is the same as for living organisms, except that medicine has no biological behaviour but instead undergoes chemical decay: the numerical particles in the model represent "droplets" of medicine, the mass of which reduces over time at a rate determined by a specified half-life. Particles are released at pen locations at specified times, according to a treatment schedule. The number of particles combined with their initial mass represents the mass of medicine required to treat a pen. The particles are then subject to advection, from the modelled flow fields, and horizontal and vertical diffusion. The choice of horizontal diffusion coefficient was informed by dye release experiments in Loch Seaforth. After 72 hours, concentrations of medicine are calculated and compared with the relevant Environmental

Quality Standard (EQS). Here, we have modelled the dispersion of azamethiphos following a treatment scenario to illustrate the quantities of medicine that disperse safely in the environment.

2.1 Model Domain and Boundary Conditions

The unstructured mesh used in the model covered Loch Seaforth and adjacent coastal waters (Figure 2). Model resolution was enhanced in the Loch Seaforth region particularly around the Mowi sites at Seaforth and Noster (Figure 3).

The mesh was not refined down to 25m specifically in the area of the pens, since dispersion is not a localised process, unlike particulate deposition, but takes place over a much wider area. However, the mesh is relatively highly resolved in the Loch Seaforth area (Figure 3) and is completely adequate for modelling dispersion of solutes. The spatial resolution of the model varied from 25m in some inshore waters to 1 km along the open boundary. In total, the model consisted of 5,419 nodes and 9,725 triangular elements.
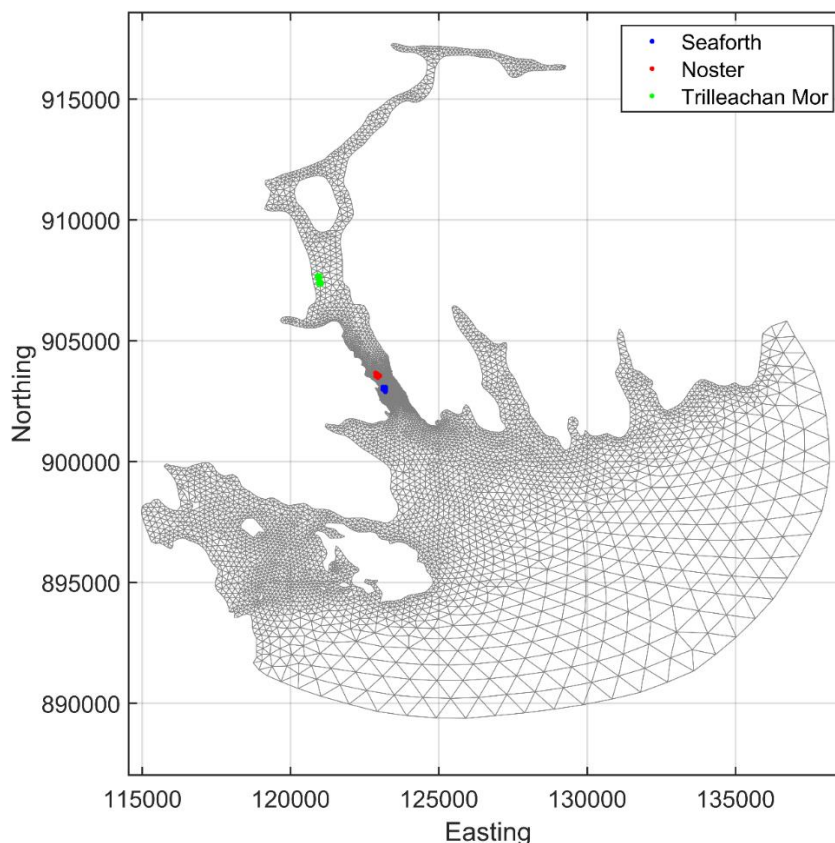
Figure 2. The model domain and mesh used in the Seaforth modelling. Farm pen locations at Seaforth (•), Noster (•) and Trilleachan Mor (•) are indicated.
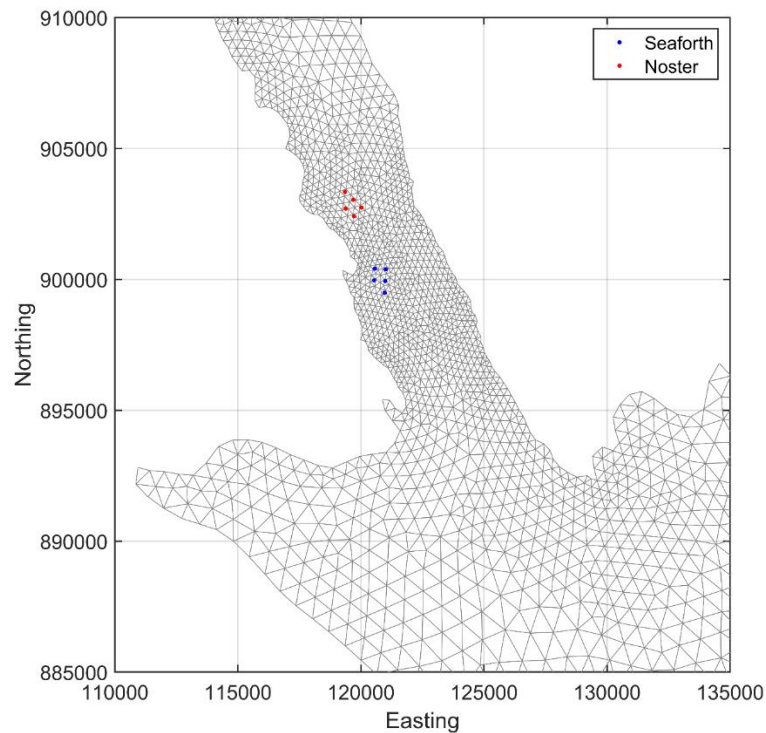
Figure 3. The model mesh in the area around the Seaforth and Noster sites. The pen locations at Seaforth (•) and Noster (•) are indicated.

Bathymetry was taken from the Marine Scotland East Coast of Lewis and Harris (ECLH) model, which has reasonably high spatial resolution around Loch Seaforth, and supplemented by a local depth survey (Figure 4). The combined data were interpolated onto the Seaforth model mesh. The combined data capture the deep channel to the northeast of the pen groups (Figure 5).

The model was forced along its open boundary by time series of sea surface height (SSH) at each boundary node for the relevant simulation periods; FVCOM appears to perform better with time series boundary forcing than when tidal constituents are used. The SSH time series were generated using the RiCOM hydrodynamic model (Walters and Casulli, 1998; Gillibrand et al., 2016b) on the ECLH grid, which was, in turn, forced by eight tidal constituents (O_1, K_1, Q_1, P_1, M_2, S_2, N_2, K_2) taken from the full Scottish Shelf model (SSM). Wind speed and direction data for the simulation periods were taken from the Stornoway meteorological station.

Stratification is expected to be moderate in this location and the model was run in 3D baroclinic mode. River flow data into Loch Seaforth was taken from measured flow data on the nearby River Laxdale, appropriately weighted for the relative catchment sizes. Ten layers in the vertical (eleven sigma levels) were used in the simulations, evenly distributed through the water column.
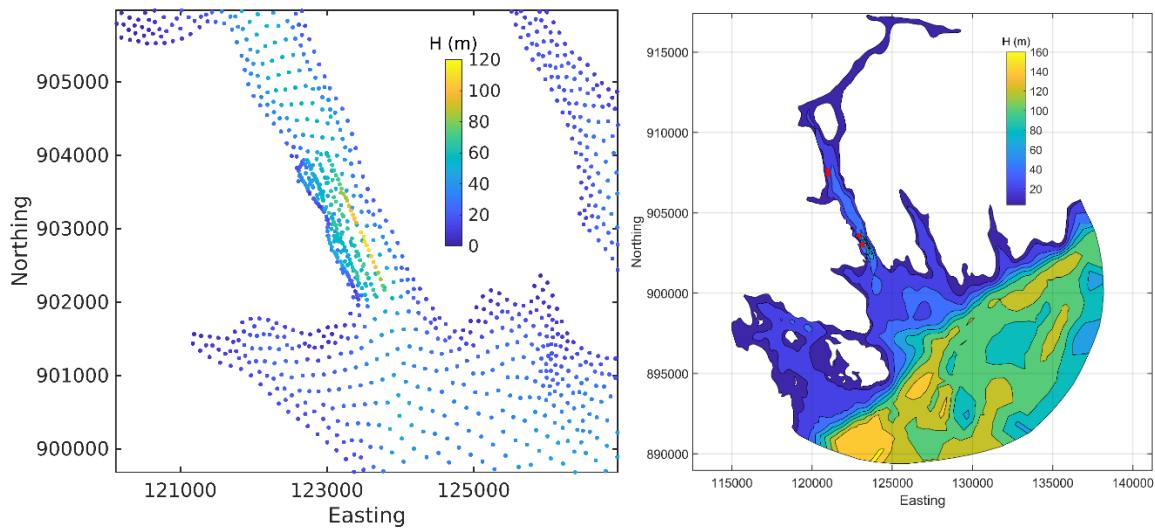
Figure 4. Spot depths from the ECLH model and the local depth survey (left) and the combined bathymetry, H (m), in the Seaforth model domain (right).
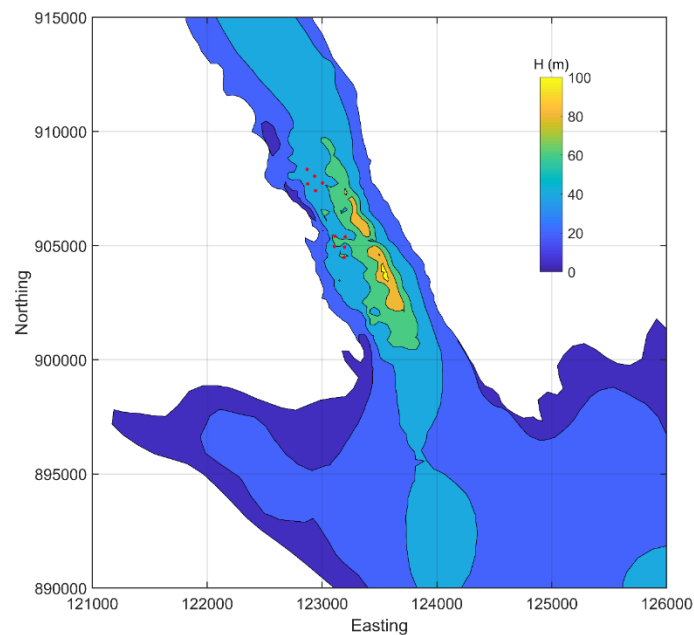
Figure 5. Localised bathymetry, H (m), around the Seaforth and Noster sites. The pen locations are marked (•).

2.2   Hydrodynamic Model Calibration

The hydrodynamic model was calibrated against current data and seabed pressure data, measured at the Seaforth site using Acoustic Doppler Current Profilers (ADCP). Data are available at two locations (
Figure 1) from 25th June – 6th September 2020 (ID347 and ID348).
The data at each location covers 73 days. Calibration was performed in a standard fashion, with bed friction adjusted to obtain the best fit against the sea surface height and current data. The model ran for the same period as the observations and the modelled surface elevation

and velocity at the three data locations were evaluated against the observed data. Details of the calibrations are given in Annex A.

Data collection using traditional ADCP deployments was challenging at the Seaforth and Noster sites. Deploying instruments close to the pens led to interference on the ADCP beams, compromising data quality. Deploying further away from the pens, in open water undisturbed by the farm pens, led to challenges with water depth which increased rapidly to the East. The deployments above (ID347 and ID348), and previous deployments not reported here, were made in water depths approaching 100m. Since data from the upper ~15% of the water column may be affected by acoustic reflection off the sea surface, deploying in these deeper depths led to no data being collected in the top ~20m.

To compensate for the challenges with the ADCP data, a second calibration exercise was performed for the dispersion model using data from dye release studies. Dye studies were performed on 25th and 28th February 2018 (see §2.5). Seven releases were made in all, and the dye patches tracked for varying lengths of time, but typically for about an hour. However, the final release was tracked for over three hours. The objective of the dye studies was to estimate horizontal diffusion coefficients, but the trajectories of the estimated patch centres were used to assess patch advection simulated by the model. This calibration exercise is reported in Appendix B.

The unptrack model uses the same unstructured mesh as the hydrodynamic model, and reads the flow fields directly from the hydrodynamic model output files. Therefore, no spatial or temporal interpolation of the current fields is required, although current velocities are interpolated to particle locations within unptrack.

2.3   Medicine Dispersion Modelling

The medicine dispersion modelling, performed using the unptrack model (Gillibrand, 2021), simulates the dispersion of patches of medicine discharged from pens following treatment using tarpaulins. The treatment scenario assumed 2 pens can be treated per day at 3- or 4-hour intervals. These are the quickest practicable schedules for installation of tarpaulins, dosage, and removal of tarpaulins for 160m pens.

To simulate the worst-case scenario, the dispersion modelling was initially conducted using flow fields over a period of six days centred on a small neap tidal range taken from the hydrodynamic model simulations. This is assumed to be the least dispersive set of ambient conditions, when the quantity of medicine able to be discharged and meet the required EQS is least. Later simulations tested dispersion during spring tides.

A treatment depth of 5.4 m was chosen as a realistic net depth during application of the medicine for 160m pens. The initial mass released per pen was calculated from the reduced pen volume and a treatment concentration of 100 µg/L, with a total mass of 5.515 kg of azamethiphos released during treatment of the whole farm (5 pens). Particles were released from random positions within a pen radius of the centre and within the 0 – 5.4 m depth range. Each numerical particle represented 10 mg of azamethiphos.

Each simulation ran for a total of 145 hours. This covered the treatment period (48 hours), a dispersion period to the EQS assessment after 120 hours (72 hours after the final treatment), and an extra 25 hours to check for chance concentration peaks. At every hour of the simulation,

particle locations and properties (including the decaying mass) were stored. Medicine concentrations were calculated from these archived results. Concentrations were calculated on a grid of 25m x 25m squares using the same depth range as the treatment depth (i.e. 0 – 5.4 m). Using a regular grid for counting makes calculating particle concentrations and presenting the results easier, and provides a known resolution of the calculated concentrations. This grid covered the area shown in Figure 3.

From the calculated concentration fields, time series of two metrics were constructed for the whole simulation:
  (i)   The maximum concentration (µg/L) anywhere on the regular grid;
  (ii)   The area (km^2) where the EQS was exceeded;

These results were used to assess whether the EQS or MAC was breached after the allotted period (72 hours after the final treatment).

Sensitivity analyses were conducted to assess the effects of:

  (i)   Medicine half-life
  (ii) Horizontal diffusion coefficient, K_H
  (iii) Vertical diffusion coefficient, K_V
  (iv) Time of release

The dispersion simulations were performed separately over neap and spring tides during 2018 (Figure 6). Further sets of simulations were performed at neap tides in 2020 to confirm the adequacy of dispersion during the weakest tides (Figure 7).
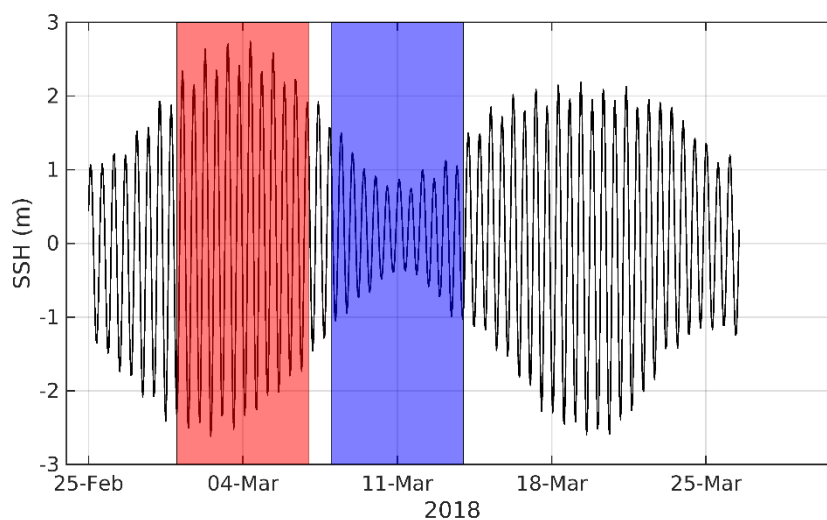
Figure 6. Sea surface height (SSH) at Seaforth from 25th Aug – 29th March 2018. The dye releases took place on 25th and 28th February. Dispersion simulations were performed over periods of neap tides (highlighted in blue) and spring tides (red).
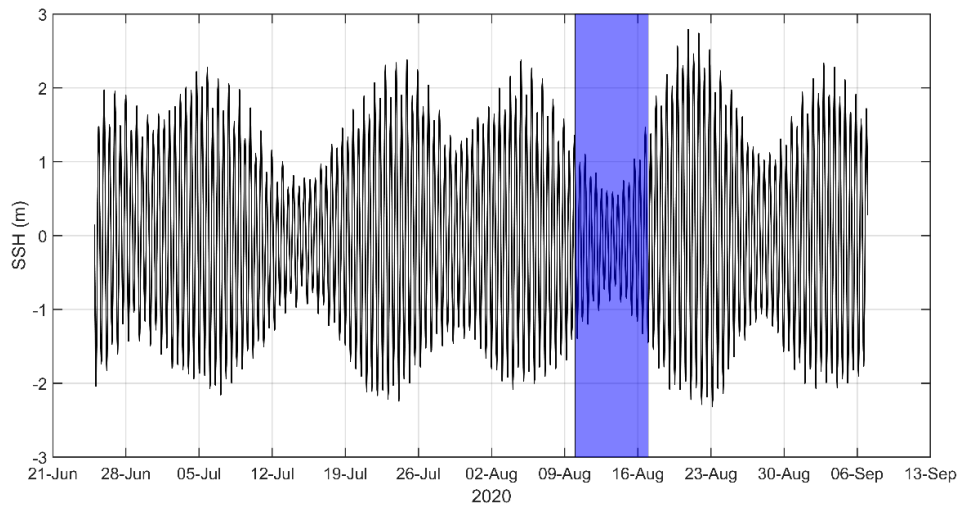
Figure 7. Measured sea surface height (SSH) at Seaforth from June – September 2020 (ID347 and ID348). Dispersion simulations were performed over the period of neap tides highlighted in blue.

2.4   Medicine Dispersion Simulations

The pens locations and details of the medicine source are listed in Table 3. The time of release is relative to the start of the neap or spring period highlighted in Figure 6 and Figure 7.

The simulations performed are listed in Table 4. All simulations used the release schedules and quantities outlined in Table 3. In Runs 4 – 9 & 17 – 22, the release schedule was set forward/back by a number of hours to investigate the effect of tidal state at the time of release on the results. Results for these simulations are still presented in terms of time relative to the first release.

Table 3. Details of the treatment at Seaforth simulated by the dispersion model. The release time is relative to the start of the neap or spring periods highlighted in Figure 6 and Figure 7.

Pen	Easting	Northing	Net Depth (m)	Treatment Mass (kg)	Release Time Schedule 1 (hr)	Release Time Schedule 2 (hr)	Release Time Schedule 3 (hr)
1	123193	902897	5.4	1.103	0	0	3
2	123197	902987	5.4	1.103	3	4	24
3	123107	902992	5.4	1.103	24	24	27
4	123202	903077	5.4	1.103	27	28	48
5	123112	903082	5.4	1.103	48	48	51

Table 4. Dispersion model simulation details for the treatment simulations of 5 pens at Seaforth.

Set	Run No.	$T_{1/2}$ (h)	K_H (m^2 s^{-1})	K_V (m^2 s^{-1})	Start Time
Neap Tides, Start Day = 12 (8th March 2018)					
1	1	134.4	0.1	0.001	00:00
2	2	213.6	0.1	0.001	00:00
	3	55.2	0.1	0.001	00:00
3	4	134.4	0.1	0.001	00:00 – 6 h
	5	134.4	0.1	0.001	00:00 – 4 h
	6	134.4	0.1	0.001	00:00 – 2 h
	7	134.4	0.1	0.001	00:00 + 2 h
	8	134.4	0.1	0.001	00:00 + 4 h
	9	134.4	0.1	0.001	00:00 + 6 h
4	10	134.4	0.05	0.001	00:00
	11	134.4	0.2	0.001	00:00
5	12	134.4	0.1	0.0025	00:00
	13	134.4	0.1	0.0050	00:00
Spring Tides, Start day = 5 (1st March 2018)					
6	14	134.4	0.1	0.001	00:00
7	15	213.6	0.1	0.001	00:00
	16	55.2	0.1	0.001	00:00
8	17	134.4	0.1	0.001	00:00 – 6 h
	18	134.4	0.1	0.001	00:00 – 4 h
	19	134.4	0.1	0.001	00:00 – 2 h
	20	134.4	0.1	0.001	00:00 + 2 h
	21	134.4	0.1	0.001	00:00 + 4 h
	22	134.4	0.1	0.001	00:00 + 6 h
9	23	134.4	0.05	0.001	00:00
	24	134.4	0.2	0.001	00:00
10	25	134.4	0.1	0.0025	00:00
	26	134.4	0.1	0.0050	00:00
Neap Tides, Start Day = 47 (10th August 2020)					
11	27	213.6	0.1	0.001	00:00
12	28	134.4	0.1	0.001	00:00
	29	55.2	0.1	0.001	00:00
13	30	134.4	0.05	0.001	00:00
	31	134.4	0.2	0.001	00:00
14	32	134.4	0.1	0.0025	00:00
	33	134.4	0.1	0.0050	00:00

2.5   Diffusion Coefficients

Selection of the horizontal diffusion parameter, K_H, was informed by dye releases conducted in Loch Seaforth by Anderson Marine Surveys Ltd. on 25th and 28th February 2018. Dye tracking studies proceed by releasing a known quantity of dye into the sea, and then attempting to map the resulting dye patch as it disperses over time by deploying a submersible fluorometer from a boat. Each survey of the patch takes a finite amount of time (typically less than 30 minutes) and is usually made up of several transects which attempt to criss-cross the patch. An estimate of horizontal diffusivity can be made from each transect, but the location of the

transect relative to the centre of the patch (and the highest concentrations) is often uncertain. Estimates of horizontal diffusivity can be made from these individual transects (Figure 8).

The analysis method is based on estimating the variance of the dye concentrations along the individual transects through the dye patch. The overall mean horizontal diffusivity from all the measurements made was 0.05 m^2 s^{-1}. There is considerable scatter in the data (Figure 8), arising from the difficulty of tracking dye in the marine environment which renders individual values highly uncertain; this difficulty is exacerbated in Scotland due to the limited quantities of dye that are permitted to be released, making it difficult to visually track the dye and take measurements that encompass the patch.
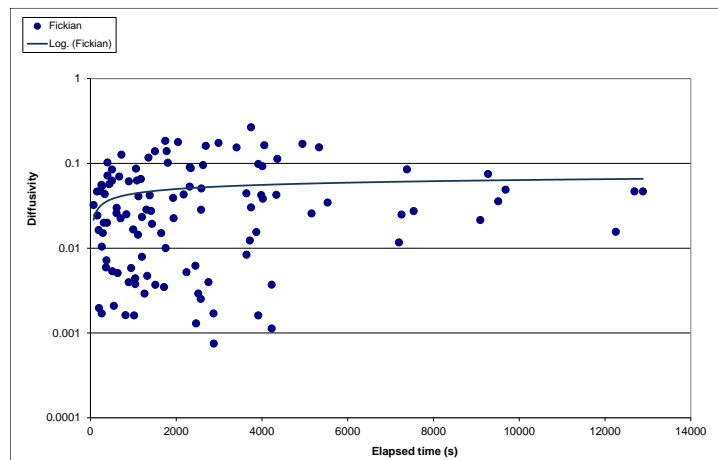
Figure 8. Estimated horizontal diffusivity (m^2 s^{-1}) from dye release experiments at Loch Seaforth on 25th and 28th February 2018. The mean diffusivity was 0.05 m^2 s^{-1}.

A second method of analysis is also presented here. According to Fickian diffusion theory (Lewis, 1997), the maximum concentration, C_{max} in a patch of dye decreases with time according to:

$$C_{max} = \frac{M}{4\pi H K_H t}$$
(1)

where M is the mass (kg) of dye released, H is a depth of water (m) over which the dye is assumed to mix vertically, K_H is the horizontal diffusivity (m^2 s^{-1}), assumed equal in x- and y-directions, and t is the time elapsed since release (s). The maximum concentration measured during each post-release survey should fall according to Equation (1) and allow an estimate of K_H to be made.

A number of dye releases have been conducted for Mowi Scotland Ltd in recent years to assess horizontal diffusivity at salmon farm sites. We have identified the maximum concentration measured in each post-release survey (each comprised of a number of individual transects) and plotted the maximum concentration against the nominal time for that survey (typically accurate to ±15 minutes). The results are shown in Figure 9. A nominal mixed surface layer depth of H = 5m was used (see also Dale et al., 2020).

The results support the notion that horizontal diffusivity in the Scottish marine environment is typically greater than 0.1 m^2 s^{-1}. The observed maximum concentrations, particularly after about 15 minutes (900s), fall faster than a diffusivity of 0.1 m^2 s^{-1} would imply, indicating greater diffusion. There is considerable uncertainty in the data, because it is difficult during dye surveys, given the limited quantities that are permitted to be released in Scotland, to visually track the dye and therefore be able to repeatedly measure the point of peak concentration. **Nevertheless, we can say that no data thus far collected infer a horizontal diffusion coefficient of less than 0.1 m^2 s^{-1}.** At periods longer than one hour (3600s), none of the data implied a horizontal diffusivity of less than 0.3 m^2 s^{-1}. We can conclude that using K$_H$ = 0.1 m^2 s^{-1} is a conservative value for modelling bath treatments over periods greater than about half-an-hour.

A similar conclusion was reached by Dale et al (2020) following dye releases conducted in Loch Linnhe and adjacent waters for a Scottish Aquaculture Research Forum study (project SARFSP012).

Most of the model simulations described in this report were conducted using a horizontal diffusion coefficient of K$_H$ = 0.1 m^2 s^{-1} which provided some conservatism in the results; however, the sensitivity of the model to K$_H$ was explored.
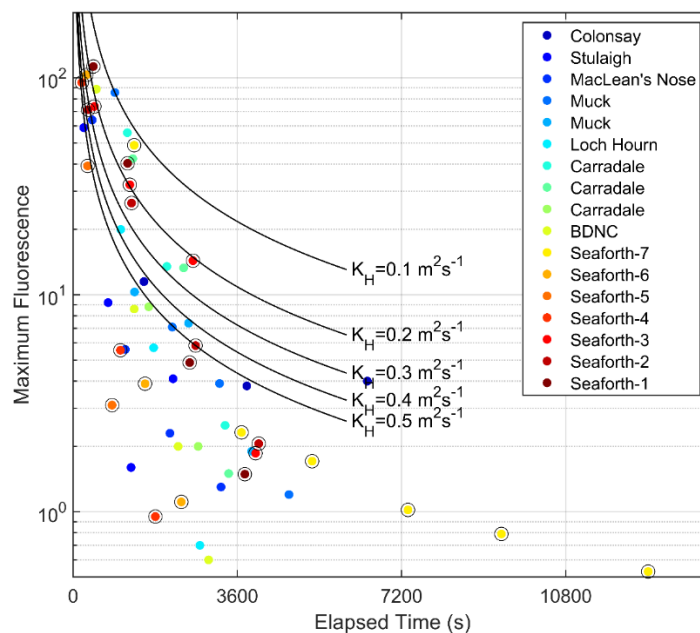
Figure 9. Maximum fluorescence measured following dye releases around Mowi farm sites during 2017 and 2018. Results from the seven releases in Loch Seaforth in February 2018 are circled (O). The releases were tracked for different lengths of time. The black lines indicate the rate at which the maximum concentration would fall at different horizontal diffusivities.

2.6 Cumulative Modelling

2.6.1 Seaforth and Noster Simultaneous Treatments

The site at Seaforth is managed by Mowi together with the neighbouring site at Noster (Figure 1). Initial modelling simulated simultaneous treatments at both sites i.e. a total of four medicine

releases per day. The releases at Noster (Table 5) exactly mirrored those at Seaforth (Table 3), since the pen configuration is identical (5 x 160m pens). Simultaneous releases at both sites were made for all simulations in Table 4. The results are reported in §3.8.1.

Table 5. Details of the treatments at Noster, in addition to those at Seaforth, simulated by the dispersion model. The release time is relative to the start of the neap or spring periods highlighted in Figure 6 and Figure 7.

Pen	Easting	Northing	Net Depth (m)	Treatment Mass (kg)	Release Time Schedule 1 (hr)	Release Time Schedule 2 (hr)	Release Time Schedule 3 (hr)
1	122944	903481	5.4	1.103	0	0	-48
2	122876	903541	5.4	1.103	3	4	-45
3	123004	903549	5.4	1.103	24	24	-24
4	122937	903608	5.4	1.103	27	28	-21
5	122870	903668	5.4	1.103	48	48	0

2.6.2   Trilleachan Mor

Finally, some simulations also including medicine releases at the other active site in Loch Seaforth with a consent to discharge azamethiphos, Trilleachan Mor, were performed. The medicine consent for Trillachean Mor, 192.7 g, is sufficient to treat one pen per day. The simulated treatments at Trilleachan Mor were initially modelled to finish at the same time as coincident treatments at Seaforth and Noster (Release Schedule 1, Table 6), such that the EQS was applied as previously. The total mass of azamethiphos released across the three sites in these simulations was 12.573 kg. Simulations were performed for spring and neap tides, using baseline conditions ($T_{1/2}$ = 134.4 h, K_H = 0.1 m^2/s, K_V = 0.001 m^2/s). Results are presented in §3.8.2.

Table 6. Details of the treatments at Trillachean Mor, in addition to those at Seaforth and Noster, simulated by the dispersion model. The release time is relative to the start of the neap or spring periods highlighted in Figure 6 and Figure 7.

Pen	Easting	Northing	Net Depth (m)	Treatment Mass (kg)	Release Time Schedule 1 (hr)
1	120910	907600	3	192.7	-120
2	120895	907687	3	192.7	-96
3	120997	907615	3	192.7	-72
4	120981	907702	3	192.7	-48
5	121040	907345	3	192.7	-24
6	121025	907432	3	192.7	0
7	120953	907330	3	192.7	24
8	120938	907416	3	192.7	48

3   RESULTS

3.1   Dispersion During Neap Tides, March 2018

A standard treatment of 5 x 160m pens, with a reduced net depth of 5.4 m (the mean depth of the 16m cone) and assuming a maximum of 2 pens could be treated per day at a treatment concentration of 0.0001 m/L, resulted in a treatment mass per pen of azamethiphos of 1.103 kg, a daily (24-h) release of up to 2.206 kg and a total treatment release of 5.515 kg over 48 hours. The dispersion of the medicine during and following treatment from Run001 is illustrated in Figure 10. After 4 hours, as the last of the first days treatments was discharged (Treatment Schedule 2), discrete patches of medicine were evident. The maximum concentration at this time was about 100 µg/L, due to the release of the second treatment. After 28 hours, as the last of the second days treatments was discharged, discrete patches of medicine from Day 2 were still evident, but the patches of medicine from the first day have rapidly dispersed and are already down to concentrations of the same order as the EQS (0.04 µg/L). The maximum concentration at this time was again about 100 µg/L, due to the release of the second treatment of the day.

The treatment schedule completed after 48 hours (2.0 days). At this stage, the medicine released on earlier days was present in a patch outside the entrance of Loch Seaforth with concentrations of the same order as the EQS. It is noticeable that dispersion of the medicine does not happen in a gradual "diffusive" manner, but is largely driven by eddies and horizontal shear in the spatially-varying velocity field, which stretches and distorts the medicine patches and enhances dispersion. After 3 days, the final treatment patches were rapidly dispersing and by 4 days, the medicine was barely evident in the loch or adjacent waters.

The time series of maximum concentration from the simulation is shown in Figure 11. The 5 peaks in concentration of ~100 µg/L following each treatment event over the first 2 days are evident. Following the final treatment after 48 hours, the maximum concentration fell steadily away (Figure 11). With a default half-life of 134.4 h (5.6 days), the maximum concentration seventy-two hours after the final treatment (time = 120 hours) was well below 0.1 µg/L, the maximum allowable concentration (MAC).

The area where the EQS of 0.04 µg/L was exceeded peaked at about 2.0 km^2 during treatment on Days 1 and 2, but had fallen below 0.5 km^2 within 21h of the final treatment; by 72 h after the final treatment, the exceeded area was zero (Figure 10 and Figure 11).

These results indicate that environmental quality standards were comfortably achieved with this treatment scenario. In the following sections, the sensitivity of the model results to the medicine half-life, diffusion coefficients and tidal state are examined.
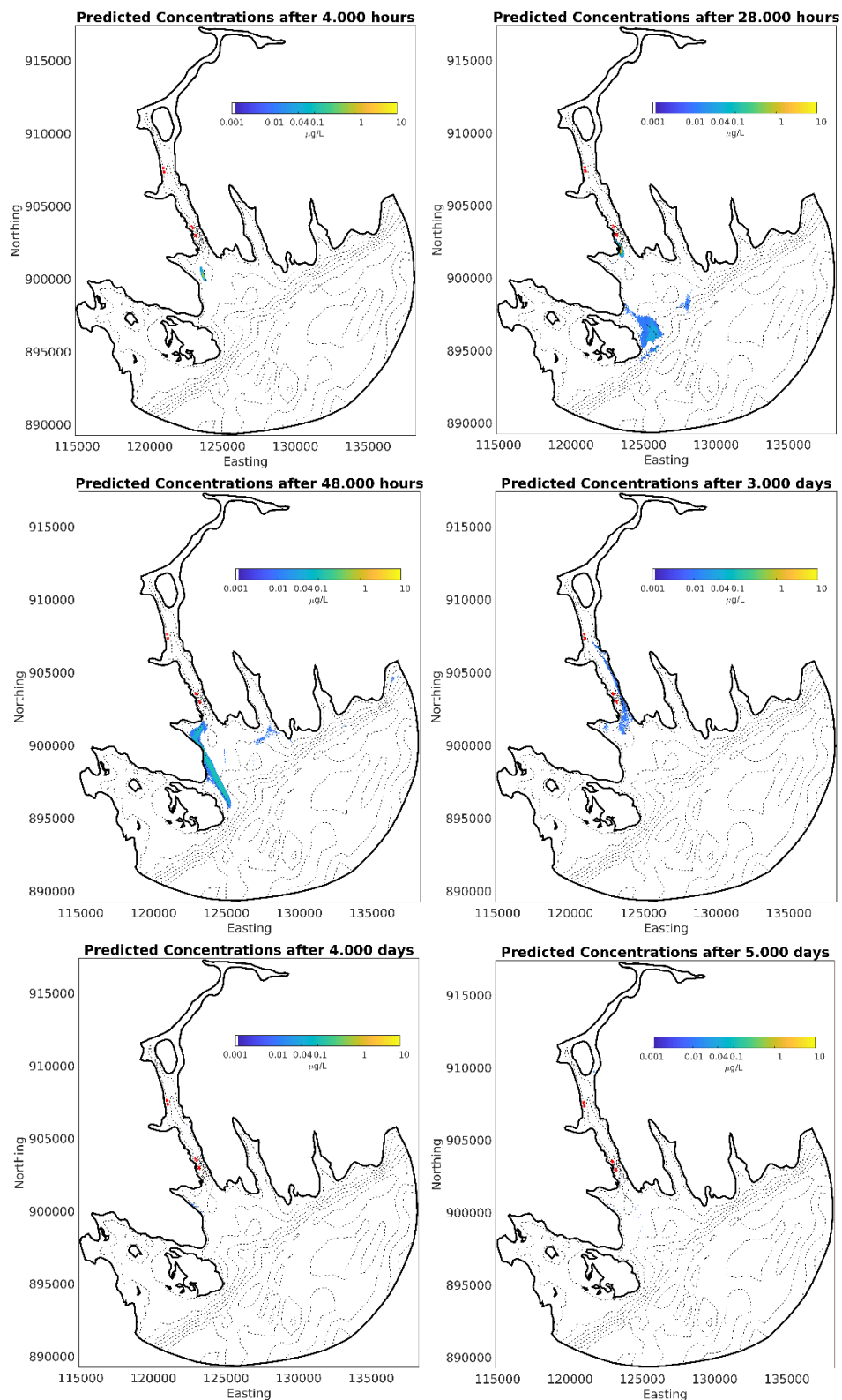
Figure 10. Predicted concentration fields (μg/L) for a dispersion simulation at neap tides after 4 hours (top left), 28 hours (top right), 48 hours (middle left), 3 days (middle right), 4 days (bottom left) and 5 days (bottom right). Pen locations for the Seaforth, Noster and Trilleachan Mor sites are indicated (•).
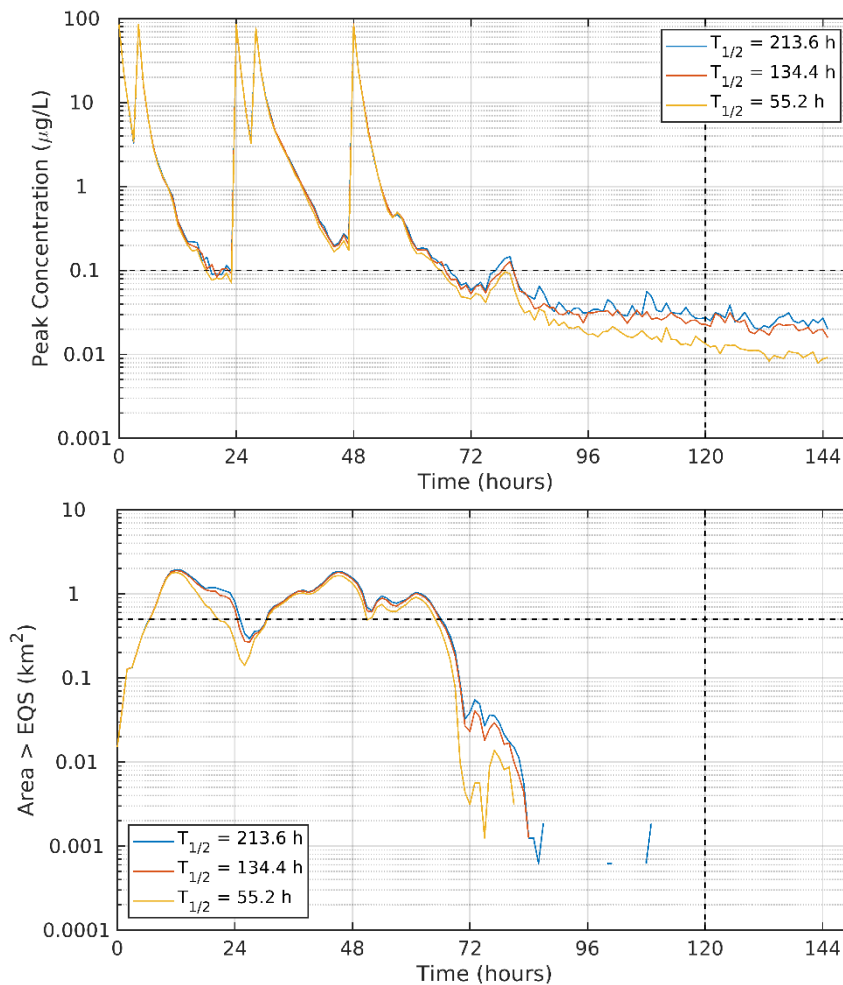
Figure 11. Time series of maximum concentration (top) and area exceeding the EQS (bottom) from the first two sets of model runs (Table 4). The model was run during neap tide in March 2018 with varying medicine half-life ($T_{1/2}$). The MAC and area limit 72 hours after the final treatment (Time = 120 h, vertical dashed line) of 0.1 µg/L and 0.5 km^2 are indicated by the horizontal dashed lines.

3.2   Sensitivity to Half-Life

Simulations with a medicine half-life of 8.9 days (213.6 h) and 2.3 days (55.2 h) were performed. In all cases, the MAC and EQS were comfortably achieved (Figure 11). The area where the EQS of 0.04 µg/L is exceeded was not affected by the different half-life, peaking at about 2.1 km^2 during treatments on Days 1 and 2, but falling well below 0.5 km^2, for all simulated half-lives, within 24 hours of the final treatment (Figure 11). The area remained below 0.5 km^2 thereafter.

3.3   Sensitivity to Release Time

The baseline simulations were repeated with the time of the releases varied by up to ±6 hours (Runs 4 – 9, Table 4), the purpose being to assess the influence, if any, of the state of the tide

on subsequent dispersion. The results show a little variability (Figure 12), however, in no case was the MAC exceeded after 120 hours, and the area where the EQS of 0.04 µg/L was exceeded fell below the limit of 0.5 km^2 within 24 hours of the final treatment. By 72 hours after the final treatment (time = 120 hours), the maximum concentration was less than 0.04 µg/L.
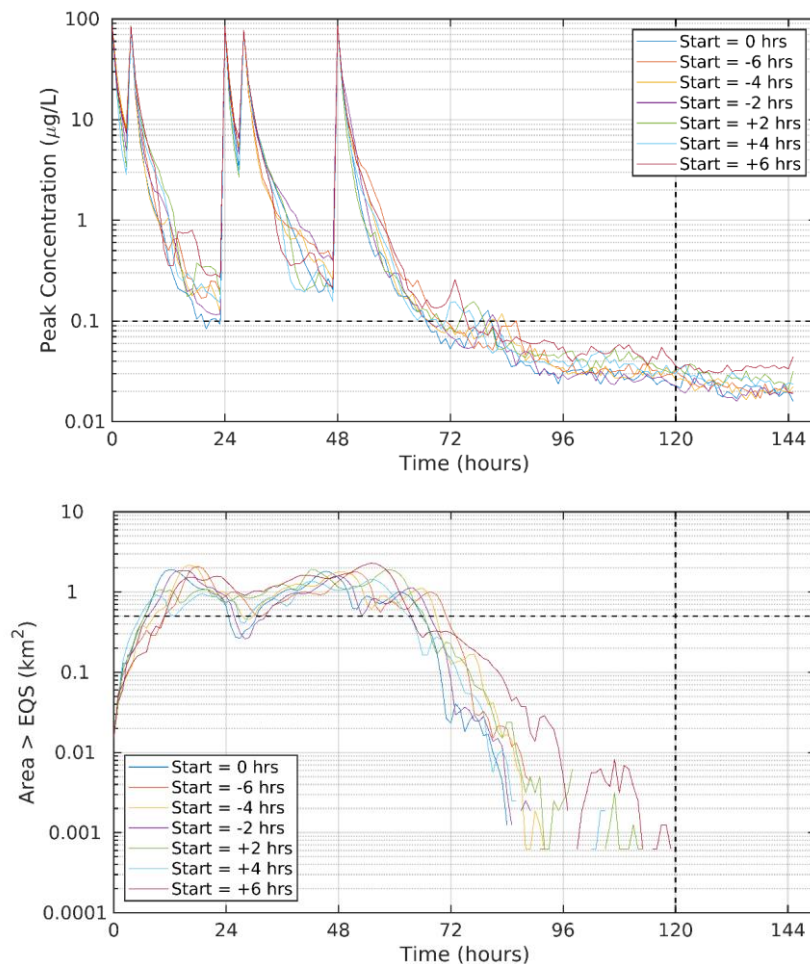
Figure 12. Time series of maximum concentration (top) and area exceeding the EQS (bottom) from the third set of model runs (Table 4). The model was run during neap tides with varying release times, relative to the baseline (Start = 0 h). The MAC and area limit 72 hours after the final treatment (Time = 120 h) of 0.1 µg/L and 0.5 km^2 are indicated by the horizontal dashed lines.

3.4   Sensitivity to Diffusion Coefficients

The model results were tested for sensitivity to the horizontal and vertical diffusion coefficients used. Although the diffusion coefficient used (K_H = 0.1 m^2 s^{-1}) is thought to be conservative, the diffusion coefficients estimated from individual transects through dye patches at Loch Seaforth had a mean value of 0.05 m^2 s^{-1}. Simulations were therefore performed with lower and higher values of K_H, specifically K_H = 0.05 m^2 s^{-1} and K_H = 0.2 m^2 s^{-1} (Table 4).

The time series of maximum concentration and area exceeding the EQS are shown in Figure 13. The time series confirm that the MAC was not exceeded after 120 hours (72 hours after the final treatment) with either the lower or higher value of K_H. The area limit of 0.5 km^2 was comfortably met in all cases. In the later stages of the simulated dispersion, the peak concentrations were not particularly sensitive to the value of the horizontal diffusion coefficient; this is because, as the patch size increases, dispersion is dominated by shear dispersion and horizontal velocity shearing rather than by eddy diffusion.

Similarly, sensitivity to the vertical diffusion coefficient, K_V, was tested. The model was slightly more sensitive to the vertical diffusion than the horizontal diffusion, but even with increased vertical diffusion, likely in the presence of wind and/or waves, the MAC and EQS conditions were very comfortably met (Figure 13).
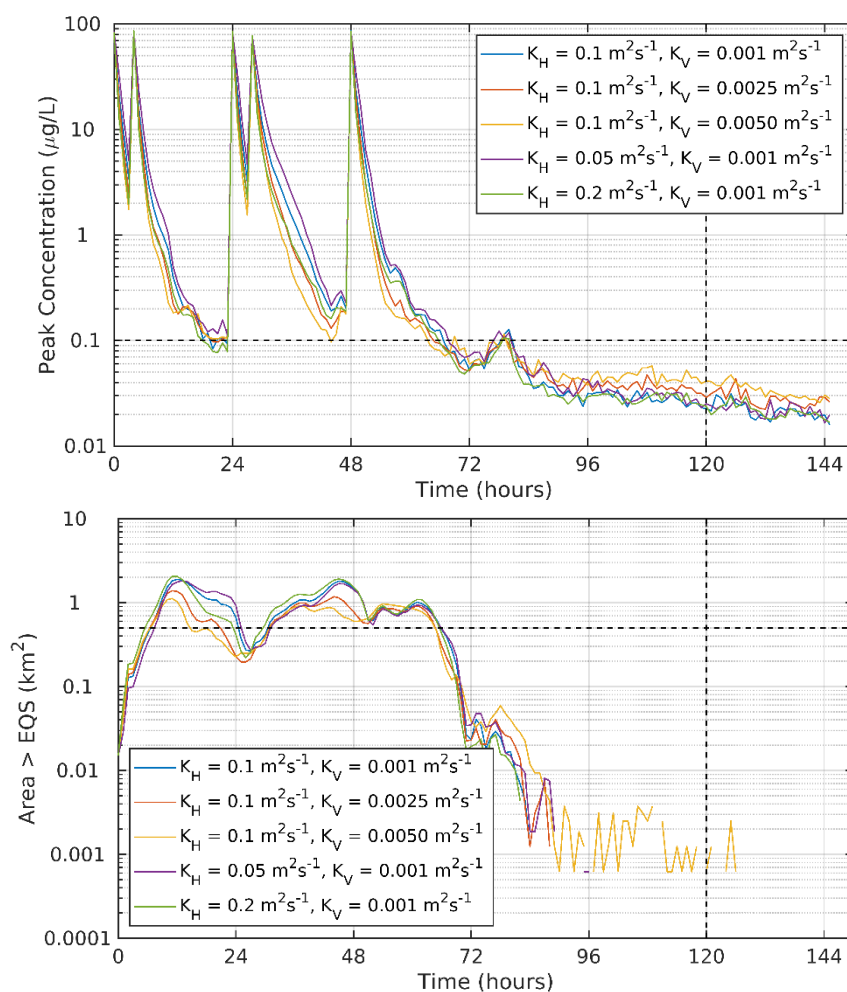
Figure 13. Time series of maximum concentration (top) and area exceeding the EQS (bottom) from the fourth set of model runs (Table 4) on treatment Schedule 2. The model was run during neap tide with varying horizontal diffusion coefficient K_H and vertical diffusion coefficient K_V. The MAC and area limit 72 hours after the final treatment (Time = 120 h) of 0.1 µg/L and 0.5 km^2 are indicated by the horizontal dashed lines.

3.5   Treatment Schedule

Runs 1 – 13 (Table 4) were repeated with both 3-hour and 4-hour treatment schedules (Table 3). The latter is a more realistic schedule for 160m cages, but the 3-hr schedule was run to demonstrate compliance. The final treatment in both schedules occurred after 48 hours, and the different treatment schedule had negligible effect on the modelled results. This is demonstrated in the section on Cumulative Modelling (§3.8.1).

3.6   Dispersion during Spring Tides, October 2018

Dispersion simulations were carried out during modelled spring tides in October 2018 (Figure 6), repeating the main set carried out for neap tides (Table 4). The same treatment scenario of 2/2/1 treatments per day respectively, at four-hour intervals was simulated, with each treatment using 1.103 kg of azamethiphos. For all medicine half-lives, start times, and horizontal and vertical diffusion coefficients simulated, both the MAC and area EQS were comfortably achieved (Figure 14 – Figure 16).
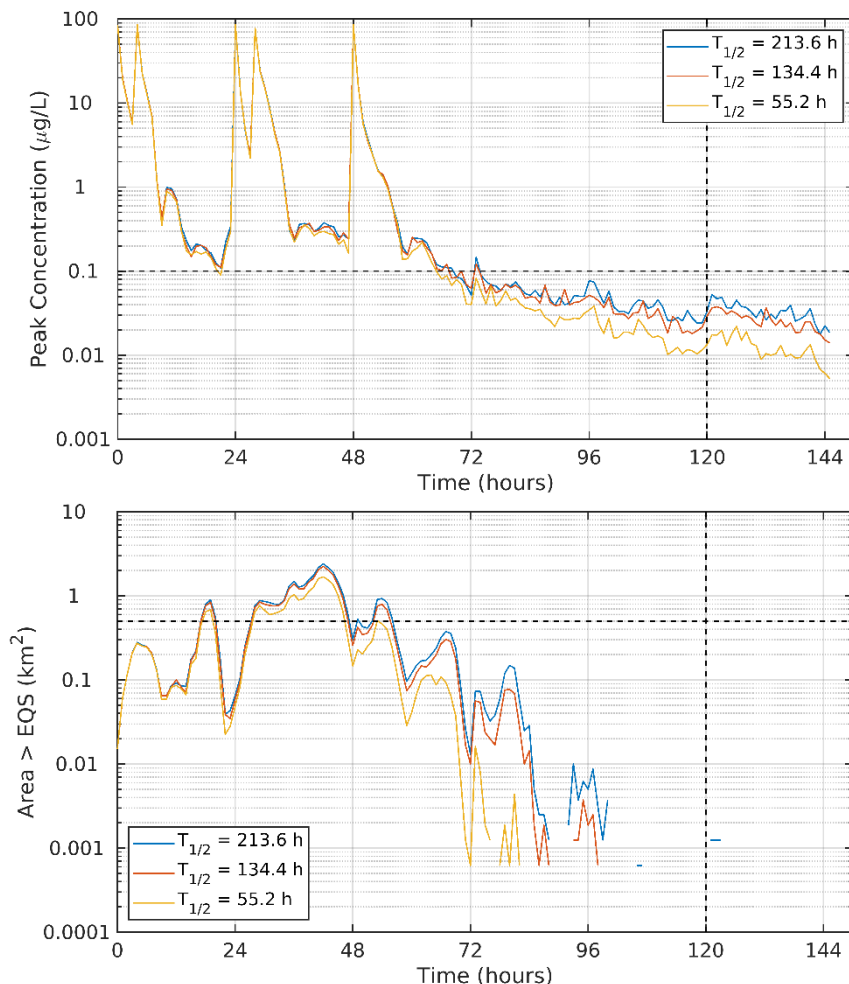
Figure 14. Time series of maximum concentration (top) and area exceeding the EQS (bottom) from simulations during spring tides in 2018 (Runs 14 – 16, Table 4). The model was run with varying medicine half-life ($T_{1/2}$). The MAC and area limit 72 hours after the final treatment (Time = 120 h, vertical dashed line) of 0.1 µg/L and 0.5 km^2 are indicated by the horizontal dashed lines.
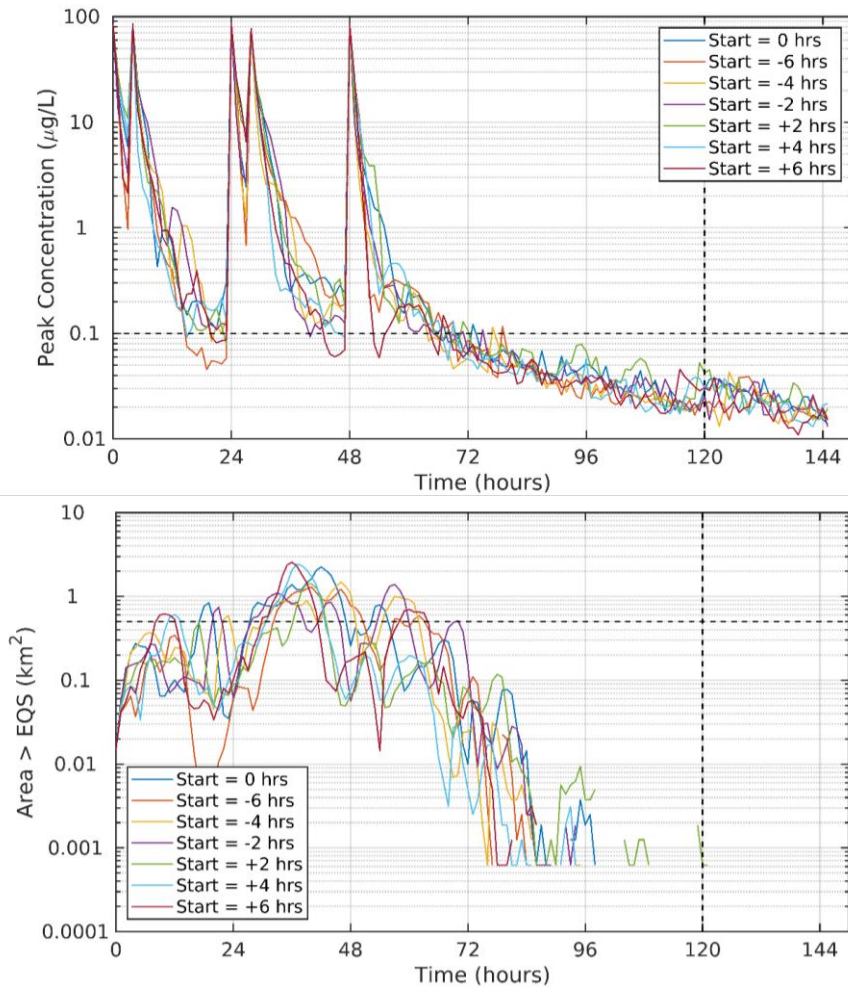
Figure 15. Time series of maximum concentration (top) and the area where concentrations exceeded the EQS (bottom) from the 6th and 8th set of model runs (Table 4). The model was run at spring tides with varying release times relative to the baseline (Start = 0 h). The MAC and area limit 72 hours after the final treatment (Time = 120 h) of 0.1 µg/L and 0.5 km² are indicated by the horizontal dashed lines.
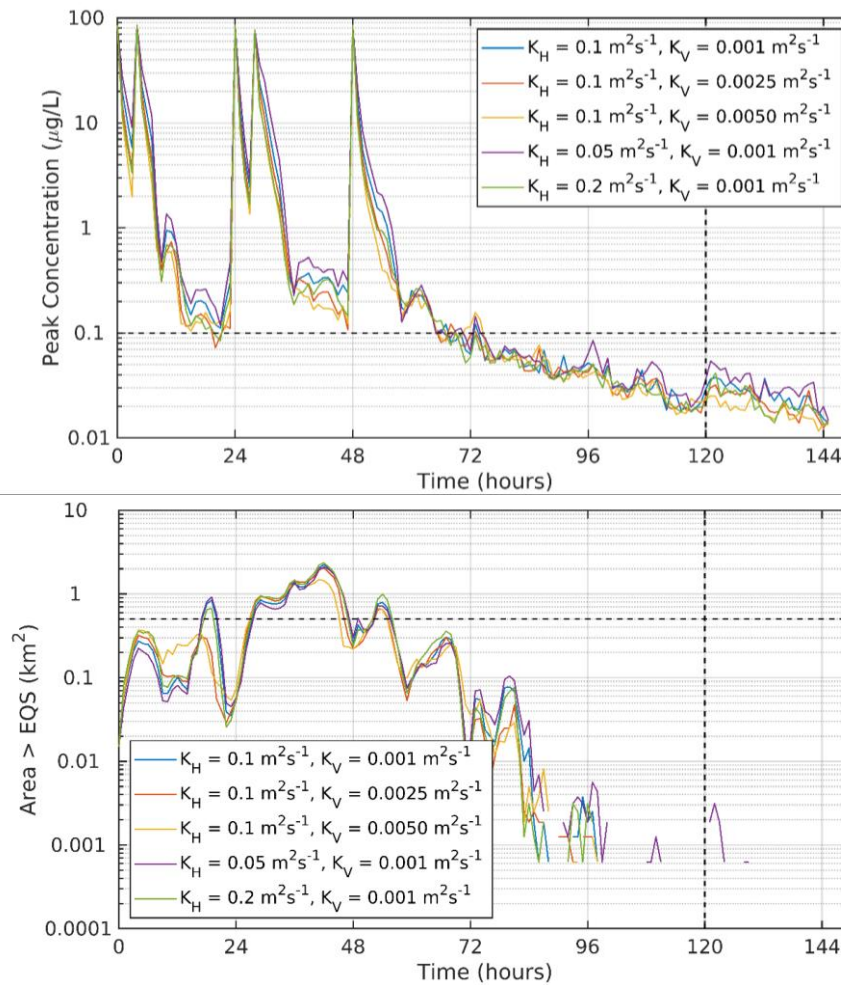
Figure 16. Time series of maximum concentration (top) and the area where concentrations exceeded the EQS (bottom) from the sixth, ninth and tenth set of model runs (varying diffusivity, Table 4). The model was run at spring tides with varying horizontal diffusion coefficient (K_H) and vertical diffusion coefficient (K_V). The MAC and area limit 72 hours after the final treatment (Time = 120 h) of 0.1 µg/L and 0.5 km^2 are indicated by the horizontal dashed lines.

3.7   Dispersion During Neap Tides, August 2020

A further set of dispersion simulations during modelled neap tides in August 2020 (Figure 7), repeating the main set carried out for neap tides (Table 4). The same treatment scenario of 2/2/1 treatments per day, respectively, at four-hour intervals was simulated, with each treatment using 1.103 kg of azamethiphos. For all medicine half-lives, start times and horizontal and vertical diffusion coefficients simulated, both the MAC and area EQS were comfortably achieved. Results from the variable half-life simulations (Figure 17) and variable diffusion coefficient sensitivity runs (Figure 18) are shown. These simulations demonstrate again that the modelled treatment regime will comfortably meet the EQS criteria.
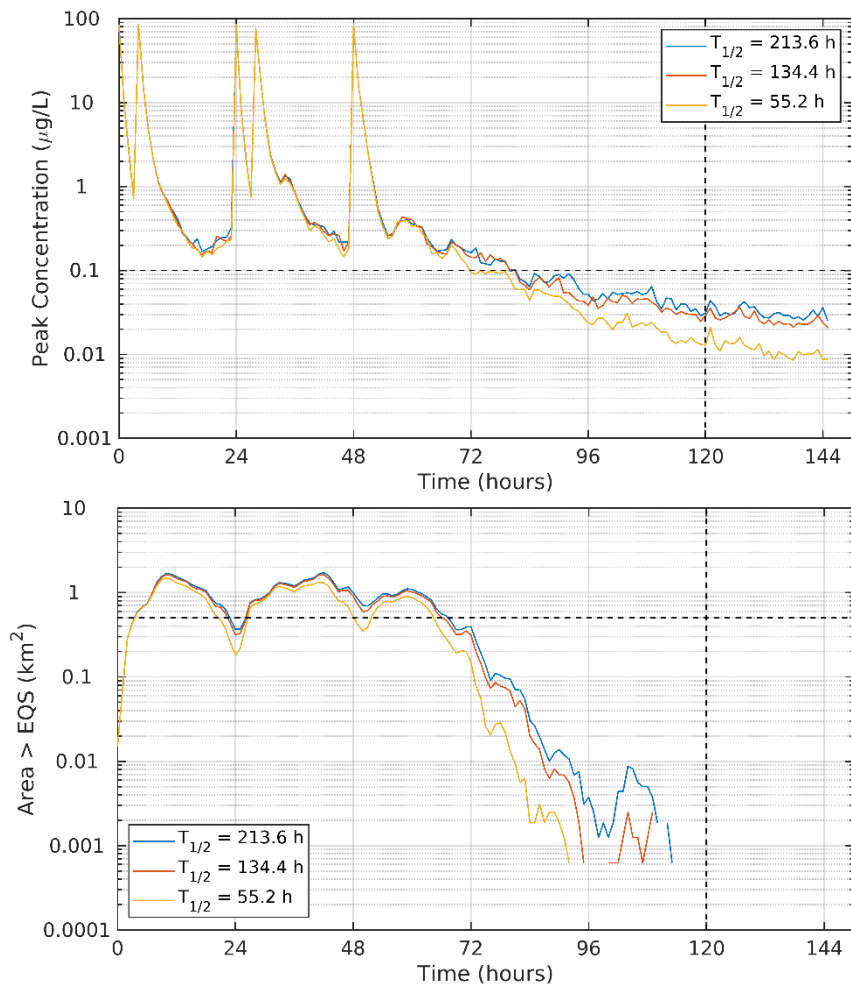
Figure 17. Time series of maximum concentration (top) and area exceeding the EQS (bottom) from simulations during neap tides in 2020 (sets 11 – 12, Table 4). The model was run with varying medicine half-life ($T_{1/2}$). The MAC and area limit 72 hours after the final treatment (Time = 120 h, vertical dashed line) of 0.1 µg/L and 0.5 km^2 are indicated by the horizontal dashed lines.
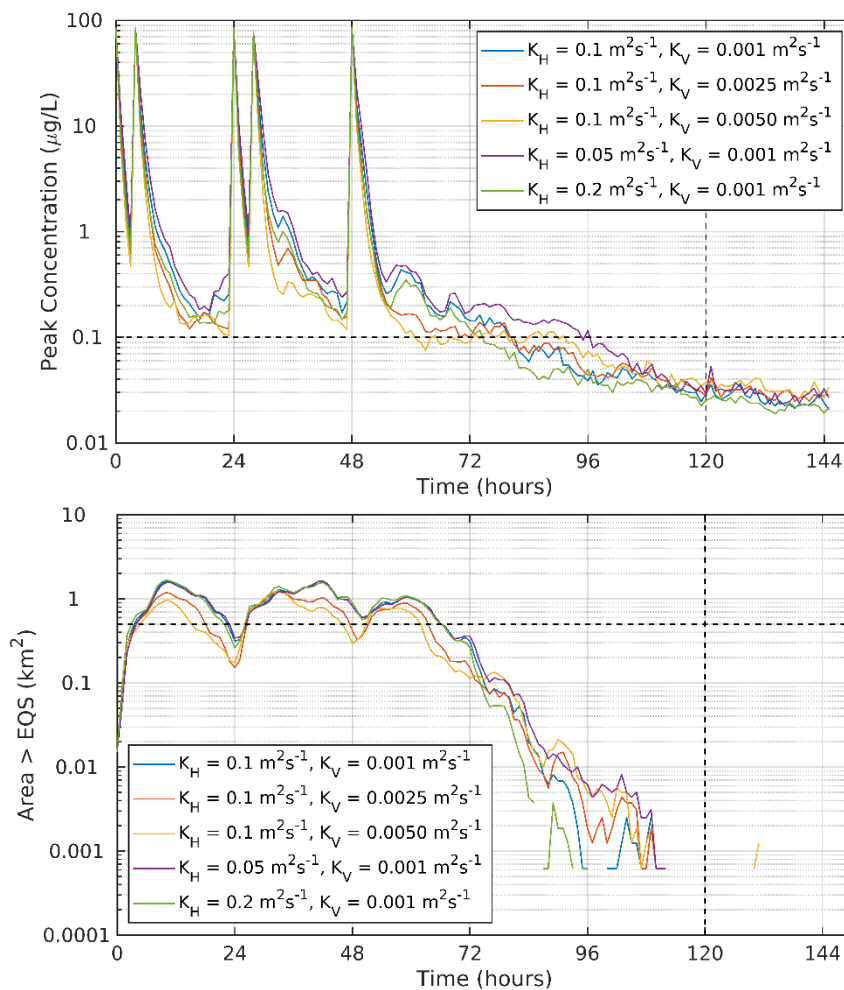
Figure 18. Time series of maximum concentration (top) and the area where concentrations exceeded the EQS (bottom) from the 11th, 13th and 14th sets of model runs (Table 4). The model was run at neap tides in August 2020 with varying horizontal diffusion coefficient (K_H) and vertical diffusion coefficient (K_V). The MAC and area limit 72 hours after the final treatment (Time = 120 h) of 0.1 µg/L and 0.5 km^2 are indicated by the horizontal dashed lines.

3.8   Cumulative Modelling

3.8.1   Seaforth and Noster Simultaneous Treatments

All simulations described in Table 4 were repeated with simultaneous treatments made at the neighbouring Noster site. In total, therefore, 2.2 kg of azamethiphos was discharged at each release (1.1 kg at each site) and a total of 4.4 kg of azamethiphos was released daily. All simulations successfully complied with environmental quality standards. A selection of results are presented below. Note that since two sites are modelled, an area EQS of 1.0 km^2 is applied, since the allowable exceedance area of 0.5 km^2 applies separately to both sites. The MAC remains unaffected by the twin treatment regime at 100 µg L^{-1}.

Figure 19 shows results from simultaneous treatments at both sites at four-hourly intervals (treatment Schedule 2, Table 3) for a release during neap tides in March 2018. The times series for different medicine half-lives times are shown.

Figure 19. Time series of maximum concentration (top) and area exceeding the EQS (bottom) from simulations of simultaneous treatments at Seaforth and Noster sites during neap tides in 2018 (Runs 1 – 3, Table 4). The model was run with varying medicine half-life ($T_{1/2}$). The MAC and area limit 72 hours after the final treatment (Time = 120 h, vertical dashed line) of 0.1 μg/L and 1.0 km^2 are indicated by the horizontal dashed lines.

Results from simulations with varying start times are shown in Figure 20. The varying start times apply to treatment regimes at both Seaforth and Noster, so the treatments at the two sites are simultaneous. Again, with a total daily release of 4.4 kg of azamethiphos, both the MAC and EQS conditions are comfortably met. Similar modelled compliance is achieved with varying horizontal and vertical diffusion coefficients (Figure 21).

Figure 20. Time series of maximum concentration (top) and area exceeding the EQS (bottom) for simultaneous treatments at Seaforth and Noster from the third set of model runs (Table 4). The model was run during neap tides in March 2018 with varying release times, relative to the baseline (Start = 0 h). The MAC and area limit 72 hours after the final treatment (Time = 120 h) of 0.1 µg/L and 1.0 km^2 (2 x 0.5 km^2) are indicated by the horizontal dashed lines.

.

Figure 21. Time series of maximum concentration (top) and area exceeding the EQS (bottom) for simultaneous treatments at Seaforth and Noster from the 4th and 5th set of model runs (Table 4) with 4-hourly treatments (treatment Schedule 2). The model was run during neap tides in March 2018 with varying horizontal (K_H) and vertical (K_V) diffusivity. The MAC and area limit 72 hours after the final treatment (Time = 120 h) of 0.1 μg/L and 1.0 km^2 (2 x 0.5 km^2) are indicated by the horizontal dashed lines.

The simulations described above used a 4-hourly treatment schedule (Schedule 2, Table 3). For comparison, Figure 22 shows results from simultaneous treatments at both sites at three-hourly intervals (treatment Schedule 1, Table 3) for the release during neap tides in March 2018. The times series for different horizontal and vertical diffusivities are shown. **The simulated treatment schedules (Table 3) had negligible impact on the results, which was found for all simulations.**
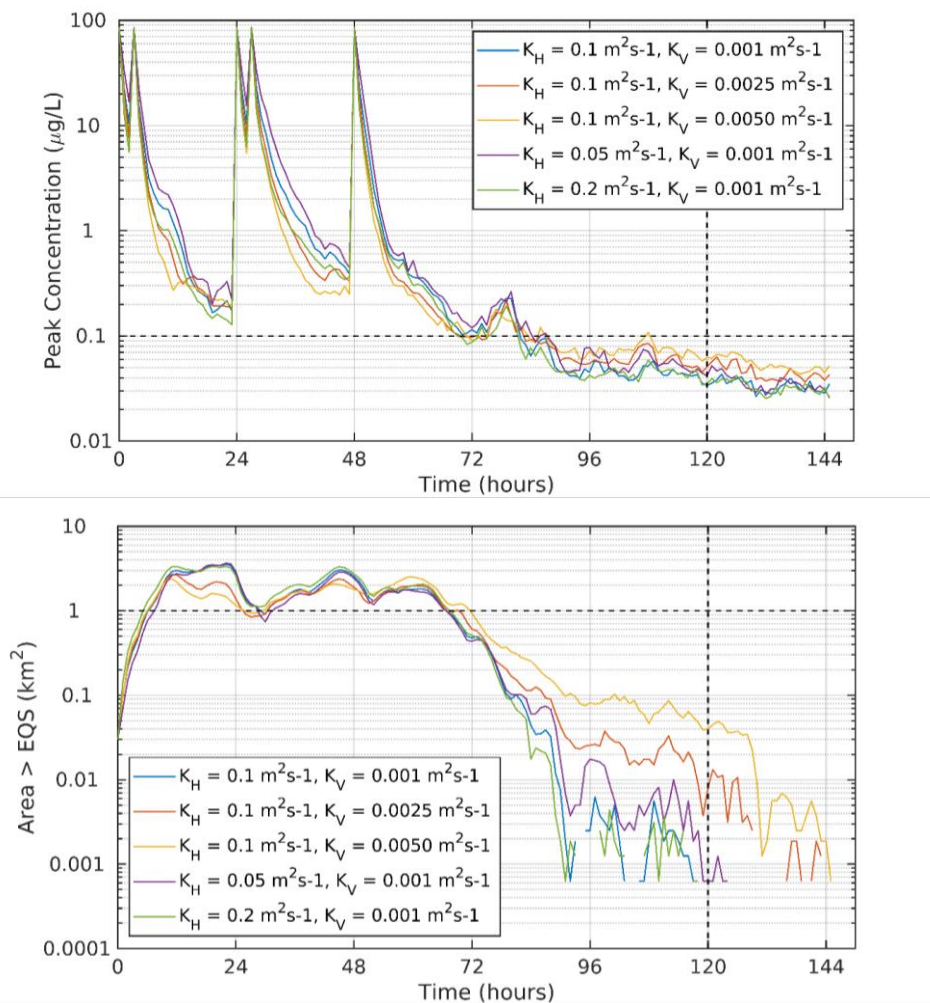
Figure 22. Time series of maximum concentration (top) and area exceeding the EQS (bottom) for simultaneous treatments at Seaforth and Noster from the 4th and 5th sets of model runs (Table 4) with 3-hourly treatments (treatment Schedule 1). The model was run during neap tides in March 2018 with varying horizontal (K_H) and vertical (K_V) diffusivity. The MAC and area limit 72 hours after the final treatment (Time = 120 h) of 0.1 µg/L and 1.0 km² (2 x 0.5 km²) are indicated by the horizontal dashed lines.

For the combined treatment simulation, with 3-hourly treatments (schedule 1), the mean concentrations over Days 2 – 5 (48 – 145 hours) are shown in Figure 23. The releases from the two sites are merged and concentrations are almost uniformly below the MAC of 0.1 µg/L, which applies after 120 hours (cf. Figure 22).
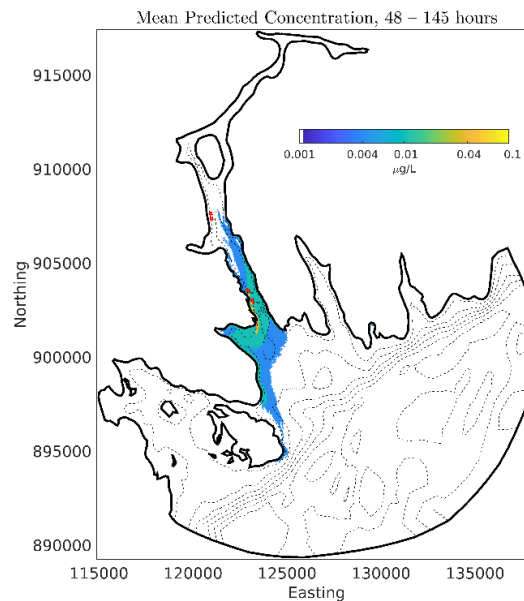
Figure 23. Mean predicted concentrations over Days 2 – 5 (time = 48 – 145 hours) for the simultaneous treatments at Seaforth and Noster, using a 3-hourly treatment schedule, . The final treatment was discharged at 48 h.

3.8.2   Trilleachan Mor

Time series of peak concentration and area exceeding the EQS for coincident treatments at Seaforth, Noster and Trilleachan Mor (Release Schedule 1, Table 6) for neap and spring tides and 3-hourly and 4-hourly treatment schedules at Seaforth and Noster are shown in Figure 24. The treatment schedule involves daily treatments at Trilleachan Mor contemporaneous with twice-daily treatments at both Seaforth and Noster i.e. up to 5 treatments per day within the loch.

The results indicate that coincident treatments at Trillachean Mor with those at Seaforth and Noster may introduce a MAC breach at spring tides.

However, that level of treatment (5 pens per day) is considered extremely unrealistic. A more realistic treatment schedule is for a maximum of two treatments per day in total at Seaforth and Noster. This could involve either two treatments per day at one site (Seaforth or Noster) or one pen at each site treated per day.

We have modelled the following scenario: daily treatments at Trilleachan Mor contemporaneous with two treatments per day in total at Seaforth/Noster. In this case, treatments at Noster started 48 hours earlier than previously (Release Schedule 3, Table 3 and Table 5), and the treatment of 10 pens at Seaforth and Noster took 5 days in total. Simulations were performed at spring and neap tides, and treatments at Seaforth and Noster were undertaken at both 3-hourly and 4-hourly intervals.

Time series of peak concentration and area exceeding the EQS for all cases are shown in Figure 25. In all cases, the EQS is now met. The reduction in the mass of azamethiphos released daily from Seaforth and Noster, from 4.4 kg to 2.2 kg per 24-hour period, allows the medicine discharged from the sites to adequately disperse.

Mean concentration fields from these simulations (Figure 26) demonstrate the reduced average concentrations resulting from treatment of 2 pens per day at Seaforth and Noster compared to 4 pens per day (together with the daily treatments at Trilleachan Mor).
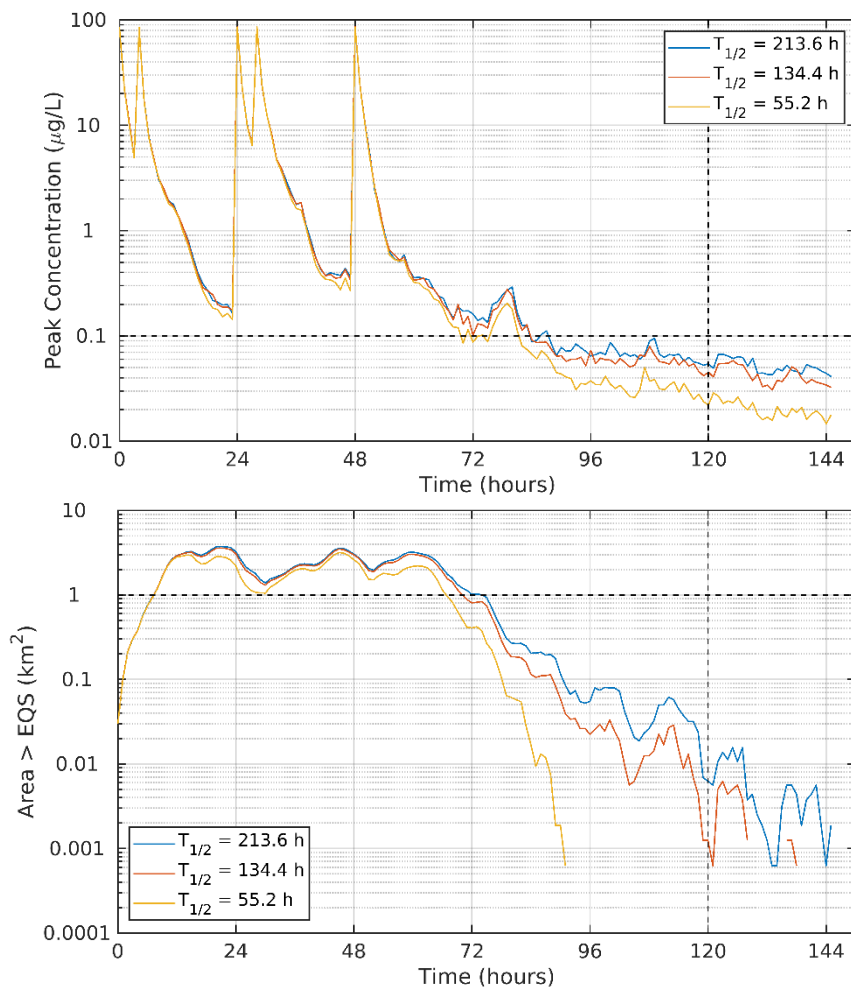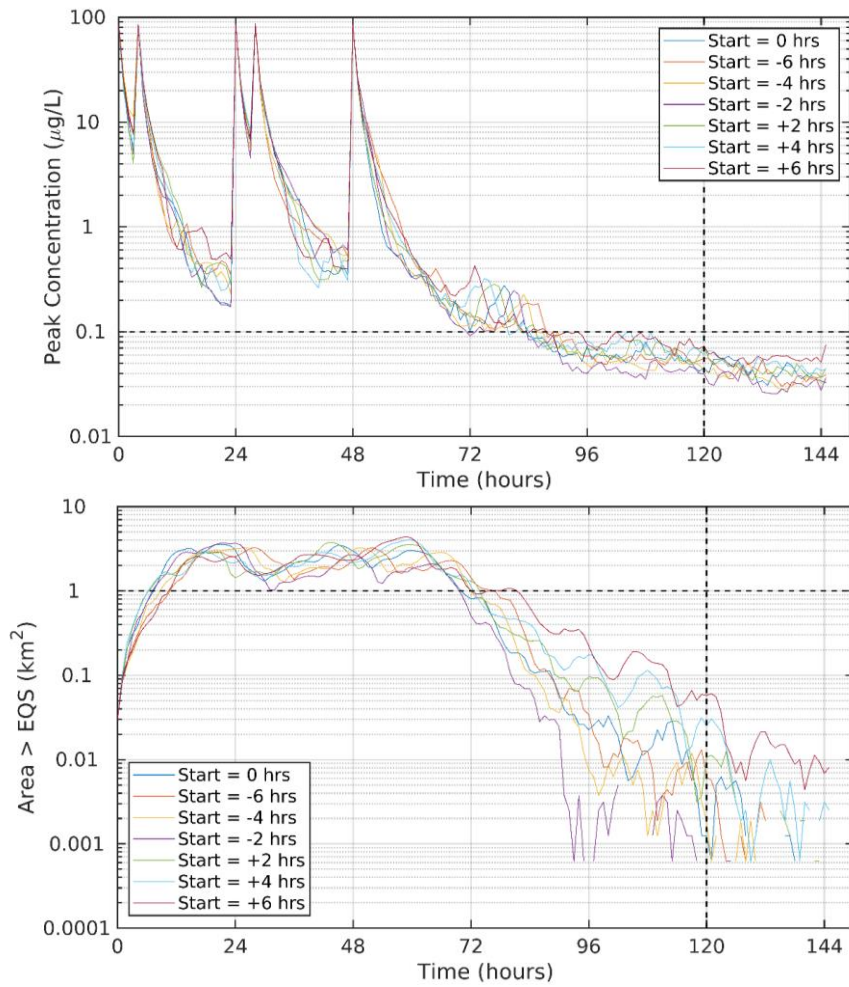

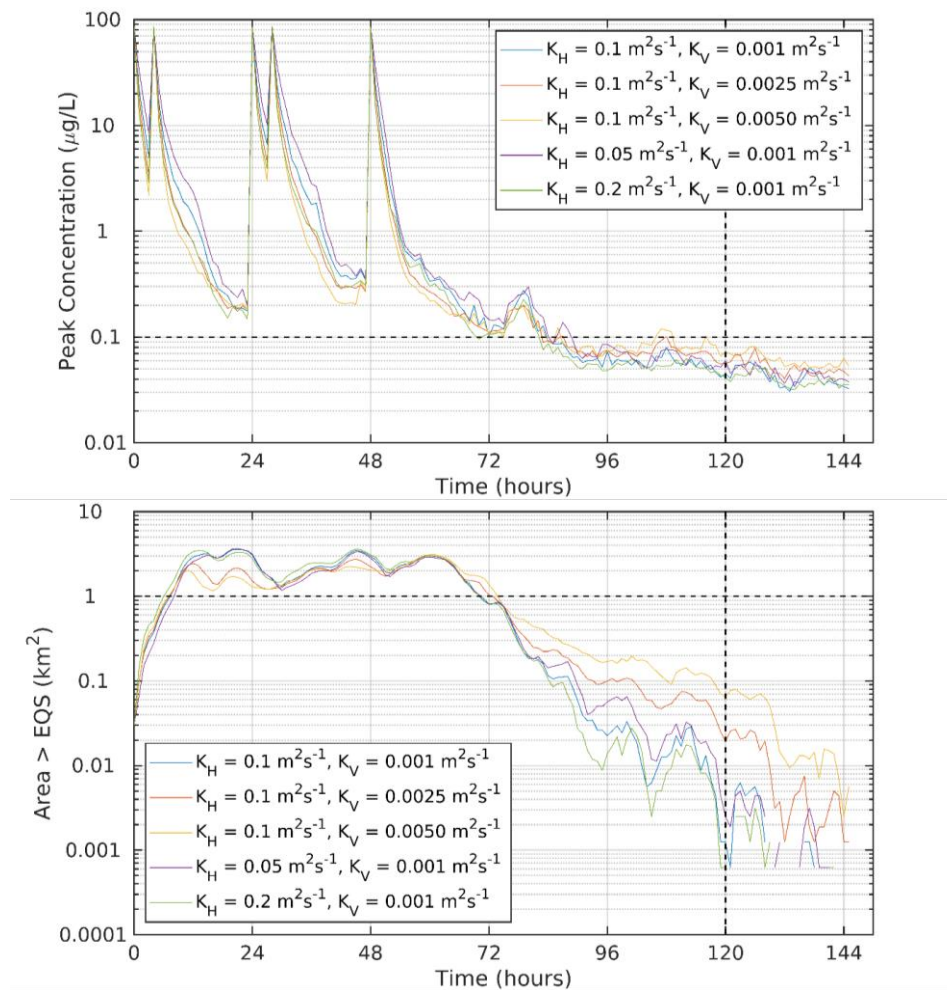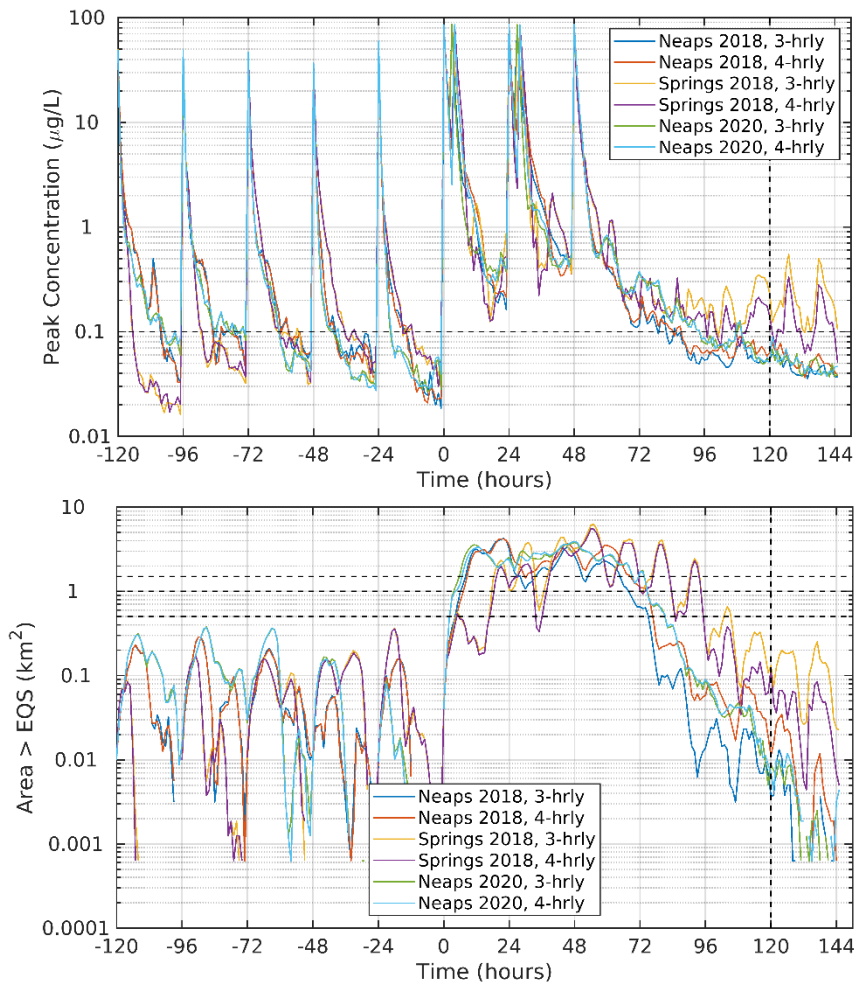Figure 24. Time series of maximum concentration (top) and area exceeding the EQS (bottom) for simultaneous treatments at Seaforth, Noster and Trilleachan Mor at neap and spring tides with 3-hourly and 4-hourly treatment schedules at Seaforth and Noster. The MAC and area limits for one, two and three sites 72 hours after the final treatment (Time = 120 h) of 0.1 µg/L and 0.5 km², 1.0 km² and 1.5 km² respectively are indicated by the horizontal dashed lines.
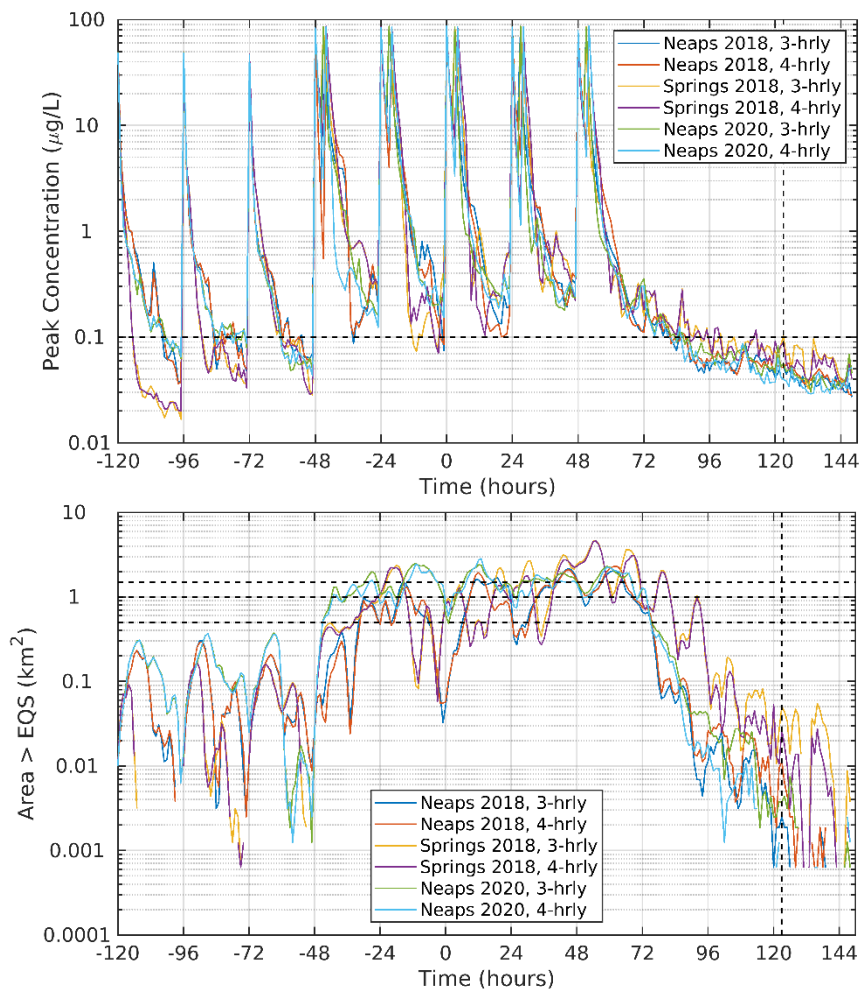
Figure 25. Time series of maximum concentration (top) and area exceeding the EQS (bottom) for contemporaneous treatments at Trilleachan Mor with two daily treatments at Seaforth/Noster at neap and spring tides with 3-hourly and 4-hourly treatment schedules. The MAC and area limits for one, two and three sites 72 hours after the final treatment (Time = 120 h) of 0.1 µg/L and 0.5 km^2, 1.0 km^2 and 1.5 km^2 respectively are indicated by the horizontal dashed lines.
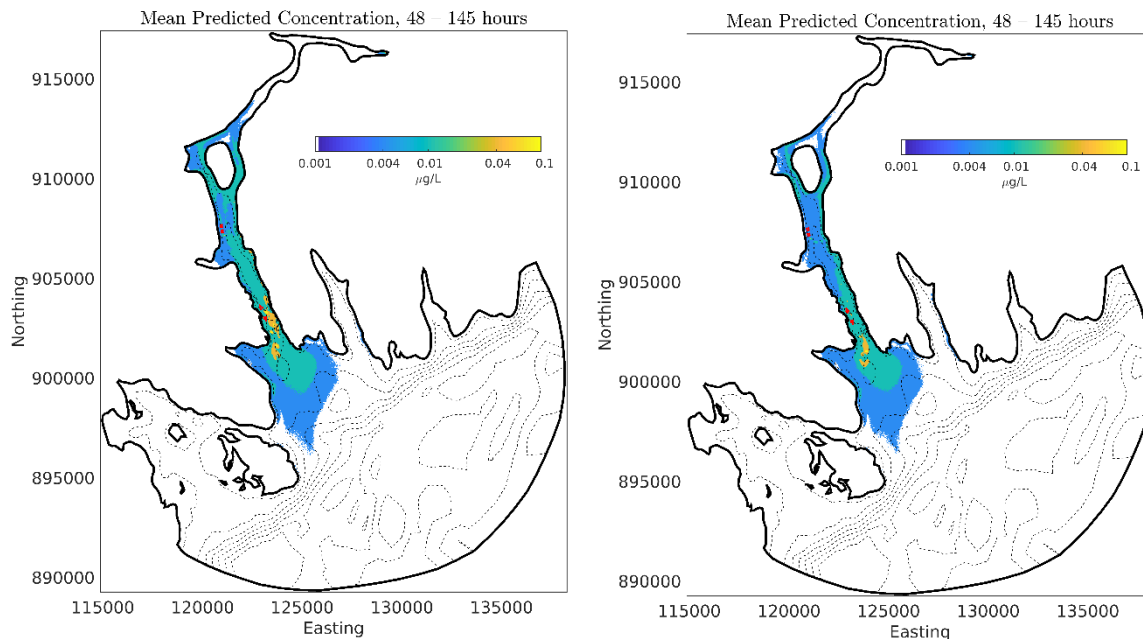
Figure 26. Mean predicted concentrations over Days 2 – 5 (48 – 145 hours) after treatments at Trilleachan Mor contemporaneously with 3-hourly treatments at Seaforth and Noster. Mean concentrations were higher when four pens per day were treated at Seaforth/Noster (left) compared to two pens per day (right). In both cases, the final treatment at all sites was discharged at 48 h.

4   SUMMARY AND CONCLUSIONS

A total of 78 dispersion simulations have been performed to assess whether bath treatments at Seaforth salmon farm will comply with pertinent environmental quality standards. Realistic treatment regimes, with 2/2/1 respective pen treatments a day at 3-hourly and 4-hourly intervals, were simulated. Each pen required 1.103 kg of azamethiphos for treatment, resulting in a maximum daily release from the site of 2.206 kg and a total discharge over 3 days of 5.515 kg. Simulations were performed separately for modelled neap and spring tides, and the sensitivity of the results to key model parameters was tested. Results are summarised in Table 7.

The model results confirmed that the treatment scenario proposed, with a daily release of no more than 2.206 kg, will consistently comply with the EQS. The peak concentration during the baseline simulation after 120 hours (72 hours after the final treatment) was consistently less than 0.1 µg/L, the maximum allowable concentration, and the area where concentrations exceeded the EQS of 0.04 µg/L was substantially less than the allowable 0.5 km². In all simulations performed, including some sensitivity testing, the EQS criteria were met. Simulations over two different neap tides from 2018 and 2020 demonstrated that the modelled treatment regime consistently complied with the relevant EQS. For the simulation during spring tides, generally greater dispersion meant that the EQS were met very comfortably. Therefore, we believe that the requested daily quantity of 2.206 kg of azamethiphos can be safely discharged without breaching the EQS.

Table 7. Summary of Results

SITE DETAILS		
Site Name: Site location: Peak biomass (T):	Seaforth Loch Seaforth 2110	
PEN DETAILS		
Number of pens: Pen dimensions: Working Depth (m): Pen group configuration:	5 160m Circumference 16 2 x 2 + 1, 90m matrix	
HYDROGRAPHIC SUMMARY	**ID347**	**ID348**
Surface Currents — Mean Speed (m/s)	0.059	0.052
Residual Speed (m/s)	0.036	0.025
Residual Direction (°G)	351	330
Tidal Amplitude Parallel (m/s)	0.085	0.079
Tidal Amplitude Normal (m/s)	0.022	0.027
Major Axis (°G)	350	325
BATH TREATMENTS		
Recommended consent mass – 3-hr Azamethiphos (g)	1103	
Recommended consent mass – 24-hr Azamethiphos (g)	2206	

The Seaforth and Noster sites are managed together. Cumulative modelling of simultaneous treatments at the two sites (4 treatment releases per day in total) demonstrated that environmental quality standards were still comfortably met.

A third site with consent to discharge azamethiphos is located at Trilleachan Mor. Cumulative modelling of coincident treatments at all three sites (up to 5 releases per day) revealed the potential for an EQS breach at spring tides. Reducing the treatment schedule at Seaforth and Noster, such that only 2 pens per day were treated (at either Seaforth or Noster, or one pen at each) together with the daily treatments at Trilleachan Mor, successfully met the MAC and EQS conditions.

It should be noted that this treatment regime, 18 pens treated in 8 consecutive days, is extremely intensive and is unlikely to occur in reality. We can be confident that more realistic treatment regimes, provided that no more than 3 pens are treated in the whole loch system per day, will not breach environmental quality standards.

The requested 24-hour mass is substantially larger than the amount predicted by the standard bath model, BathAuto, but the latter is known to be highly conservative, because it does not account for horizontal shearing and dispersion of medicine patches due to spatially-varying current fields, processes which are known to significantly influence dispersion over times scales greater than a few hours (e.g. Okubo, 1971; Edwards, 2015), as illustrated in Figure 10.

5   REFERENCES

Burchard, H., 2002. Applied turbulence modeling in marine waters. Springer:Berlin-Heidelberg-New York-Barcelona-Hong Kong-London-Milan Paris-Tokyo, 215pp.

Chen, C., H. Liu, and R.C. Beardsley, 2003. An unstructured, finite-volume, three-dimensional, primitive equation ocean model: Application to coastal ocean and estuaries. J. Atmos. Ocean. Tech., 20, 159 – 186.

Dale. A., Allen. C., Venables. E., Beaton. J. & Aleynik. D. (2020). Dye tracer dispersion studies in support of bath treatment models for fish farms (2020). A study commissioned by the Scottish Aquaculture Research FoSeaforth (SARF). http://www.sarf.org.uk/SARFSP012.pdf

Edwards, A., 2015. A note on dispersion in West Scottish coastal waters. A Report for Benchmark Animal Health. September 2015, 55pp.

Gillibrand, P.A., 2021. Unptrack User Guide. Mowi Scotland Ltd., February 2021, 31 pp..

Gillibrand, P.A., B. Siemering, P.I. Miller and K. Davidson, 2016a. Individual-Based Modelling of the Development and Transport of a Karenia mikimotoi Bloom on the North-West European Continental Shelf. Harmful Algae, DOI: 10.1016/j.hal.2015.11.011

Gillibrand, P.A., Walters, R.A., and McIlvenny, J., 2016b. Numerical simulations of the effects of a tidal turbine array on near-bed velocity and local bed shear stress. *Energies*, vol 9, no. 10, pp. 852. DOI: 10.3390/en9100852

Gillibrand, P.A. and K.J. Willis, 2007. Dispersal of Sea Lice Larvae from Salmon Farms: A Model Study of the Influence of Environmental Conditions and Larval Behaviour. Aquatic Biology, 1, 73-75.

Lewis, R. 1997. Dispersion in Estuaries and Coastal Waters. John Wiley & Sons, 332 pp.

Marine Scotland 2016. The Scottish Shelf Model. Marine Scotland. http://marine.gov.scot/themes/scottish-shelf-model

Okubo, A., 1971. Oceanic diffusion diagrams. Deep-Sea Research, 18, 789 – 802.

SEPA, 2019. Aquaculture Modelling. Regulatory modelling guidance for the aquaculture sector. Scottish Environment Protection Agency, Air & Marine Modelling Unit, June 2019, 68pp.

Walters, R.A.; Casulli, V., 1998. A robust, finite element model for hydrostatic surface water flows. Comm. Num. Methods Eng., 14, 931–940.

Willis, K.J, Gillibrand, P.A., Cromey, C.J. and Black, K.D., 2005. Sea lice treatments on salmon farms have no adverse effect on zooplankton communities: A case study. *Marine Pollution Bulletin*, 50, 806 – 816.

ANNEX A. HYRODYNAMIC MODEL DESCRIPTION

A.1   Model Description

FVCOM (Finite Volume Community Ocean Model) is a prognostic, unstructured-grid, finite-volume, free-surface, 3-D primitive equation coastal ocean circulation model developed by the University of Massachusetts School of Marine Science and the Woods Hole Oceanographic Institute (Chen et al., 2003). The model consists of momentum, continuity, temperature, salinity and density equations and is closed physically and mathematically using turbulence closure submodels. The horizontal grid is comprised of unstructured triangular cells and the irregular bottom is presented using generalized terrain-following coordinates. The General Ocean Turbulent Model (GOTM) developed by Burchard's research group in Germany (Burchard, 2002) has been added to FVCOM to provide optional vertical turbulent closure schemes. FVCOM is solved numerically by a second-order accurate discrete flux calculation in the integral form of the governing equations over an unstructured triangular grid. This approach combines the best features of finite-element methods (grid flexibility) and finite-difference methods (numerical efficiency and code simplicity) and provides a much better numerical representation of both local and global momentum, mass, salt, heat, and tracer conservation. The ability of FVCOM to accurately solve scalar conservation equations in addition to the topological flexibility provided by unstructured meshes and the simplicity of the coding structure has make FVCOM ideally suited for many coastal and interdisciplinary scientific applications.

The mathematical equations are discretized on an unstructured grid of triangular elements which permits greater resolution of complex coastlines, such as typically found in Scotland. Therefore greater spatial resolution in near-shore areas can be achieved without excessive computational demand.

A.2   Configuration and Boundary Forcing for Loch Seaforth

The unstructured mesh used in the model covered Loch Seaforth and adjacent coastal waters (Figure 2). Model resolution was enhanced in the Loch Seaforth region particularly around the Mowi sites at Seaforth and Noster (Figure 3).

The mesh was not refined down to 25m specifically in the area of the pens, since dispersion is not a localised process, unlike particulate deposition, and takes place over a much wider area. However, the mesh is relatively highly resolved in the Loch Seaforth area (Figure 3) and is completely adequate for modelling dispersion of solutes. The spatial resolution of the model varied from 25m in some inshore waters to 1 km along the open boundary. In total, the model consisted of 5,419 nodes and 9,725 triangular elements.

Bathymetry was taken from the Marine Scotland East Coast of Lewis and Harris (ECLH) model, which has reasonably high spatial resolution around Loch Seaforth, and supplemented by a local depth survey (Figure 4). The combined data were interpolated onto the Seaforth model mesh. The combined data capture the deep channel to the northeast of the pen groups (Figure 5).

The model was forced along its open boundary time series of sea surface height (SSH) at each boundary node for the relevant simulation periods; FVCOM appears to perform better with time

series boundary forcing than when tidal constituents are used. The SSH time series were generated using the RiCOM hydrodynamic model (Walters et al., 2010; Gillibrand et al., 2016b) on the ECLH grid, which was, in turn, forced by eight tidal constituents (O_1, K_1, Q_1, P_1, M_2, S_2, N_2, K_2) taken from the full Scottish Shelf model (SSM). Wind speed and direction data were taken from the Stornoway meteorological station.

Stratification is expected to be moderate in this location and the model was run in 3D baroclinic mode. River flow data into Loch Seaforth was taken from measured flow data on the nearby River Laxdale, appropriately weighted for the relative catchment sizes. Ten layers in the vertical (eleven sigma levels) were used in the simulations, evenly distributed through the water column.

A.3   Model Calibration and Evaluation

For the current study, the model was further calibrated against hydrographic data collected in the region of the farm site in 2020. The data are described in the relevant hydrographic reports. In June 2020, two Acoustic Doppler Current Profilers (ADCPs) were deployed close to the Seaforth and Noster farm sites (Figure A.1) until September 2020. In all, 148 days of current data were used in this application. The ADCP deployments provided both current velocity and seabed pressure data, which were used to calibrate the modelled velocity and sea surface height. A further validation of the coupled hydrodynamic-particle tracking modelling system was performed using tracks of dye patches from dye release studies performed in 2018 (Appendix B).

For model simulations, the model was "spun-up" for five days with boundary forcing ramped up from zero over a period of 48 hours. The model state at the end of the 72-hour spin-up period was stored, and the main simulations "hot-started" from this state:

1. Spin-up: 20th June – 25th June 2020
2. Main Run: 25th June – 7th September 2020

Model performance is assessed using three metrics: the mean absolute error (MAE), the root-mean-square error (RMSE) and the model skill (d_2). The first two are standard measures of model accuracy; the third, d_2, is taken from Willmott et al. (1985) and lies in the range $0 \leq d_2 \leq 1$, with $d_2 = 0$ implying zero model skill and $d_2 = 1$ indicating perfect skill.

Table A.1. Parameter values chosen for the FVCOM model during the calibration simulations.

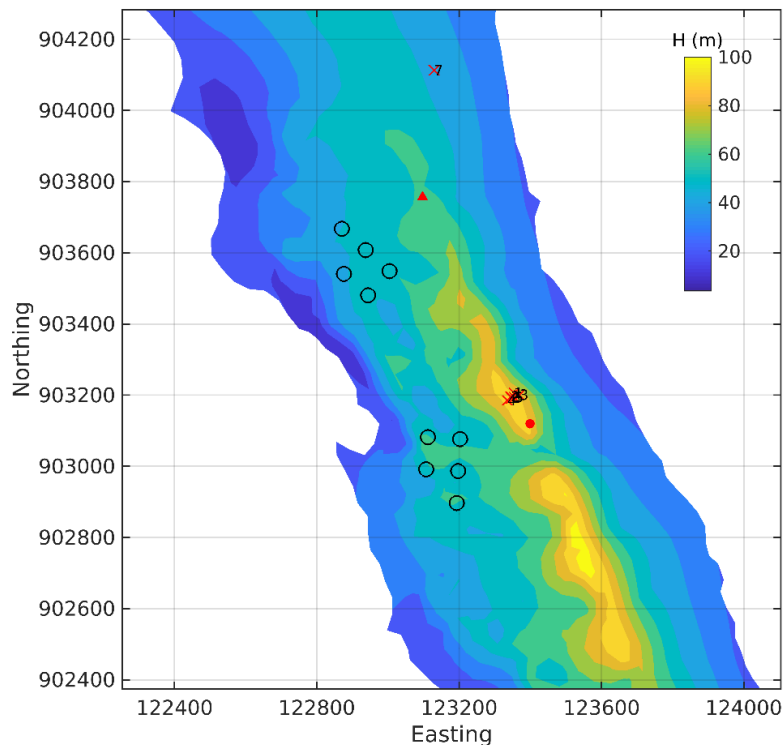| Parameter Description	Value
Bottom roughness lengthscale, z_0	0.01
Horizontal diffusion coefficient ($m^2\ s^{-1}$)	0.1
Horizontal viscosity coefficient ($m^2\ s^{-1}$)	1.0
Number of vertical levels	11
Barotropic model time step (s)	1.0
Baroclinic model time step (s)	10.0

Figure A.1. Locations of the ADCP deployments ID347 (▲) and ID348 (●) relative to the 10 pens at the Seaforth and Noster sites (O). The locations of the 7 dye releases on 25th and 28th February are also indicated (X).

The calibration used observed depth and current velocity from the ADCP location to compare with modelled sea surface height (SSH) and velocity (ADCP deployments ID347 and ID348). The model was calibrated by varying the value of the bottom roughness lengthscale, z_0, which determines the frictional effect of the seabed on the flow. Simulations were performed with a range of values of z_0, varying over the range 0.001 m ≤ z_0 ≤ 0.1 m. Some further refinement of the model simulations was performed by modifying the horizontal viscosity and diffusion coefficients. After a number of simulations, a final parameter set was selected (Table A.1).

A.3.1 June – September 2020, Noster (ID347)

The results of the calibration exercise are presented in Figures A.2 – A.4 and Table A.3. At the ADCP location, the sea surface height was accurately modelled, with model skill of 0.99. The mean absolute error (MAE) and root-mean-square error (RMSE) values of 0.16 m and 0.2 respectively are about 3% and 4% of the spring tide range respectively.

North and east components of velocity at the ADCP location were satisfactorily reproduced by the model, with values of the model skill, d_2, of about 0.5 – 0.7 for the East component and values exceeding 0.8 for the North component (Figure A.3, Table A.3). The scatter plots shown in Figure A.4 demonstrate that the modelled currents were broadly of the same magnitude and direction as the observed data.
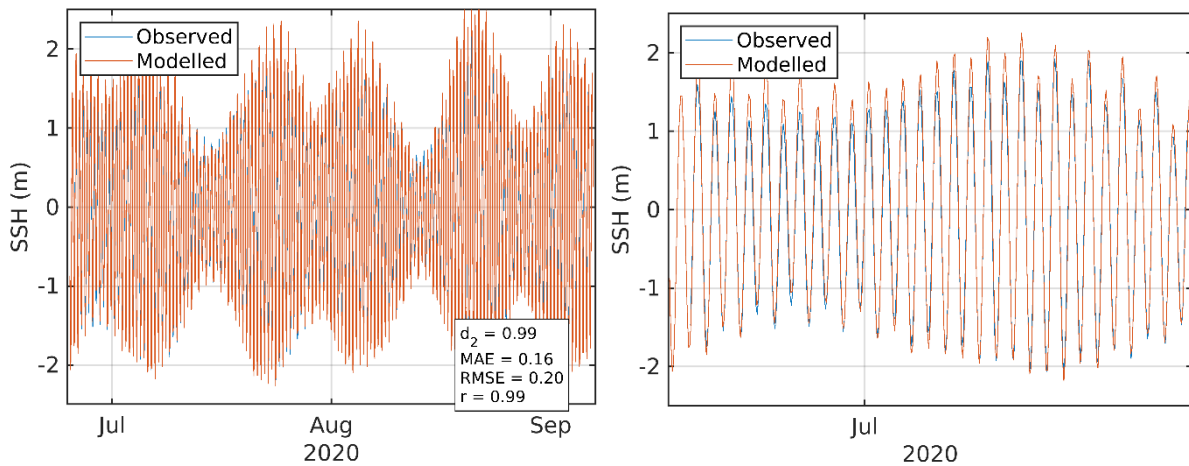
Figure A.2. Comparison between observed and modelled sea surface height from June – September 2020 at the Noster ADCP location (ID347) using model parameter values from Table A. Both the full record (left) and a subset of 15 days (right) are shown. Observed data are in blue, model results in red.

Table A.2. Model performance statistics for sea surface height (SSH) at Noster (ADCP deployment ID347) and Seaforth (ID348) for June – September 2020.

	ID347	ID348
Skill, d_2	0.99	0.99
Mean Absolute Error (MAE)	0.16 m	0.14 m
Root-Mean-Square Error (RMSE)	0.20 m	0.17 m

Figure A.3. Comparison between observed and modelled East (top) and North (bottom) components of velocity at three depths at the Noster ADCP location (ID347) for June – September 2020. Observed data are in blue, model results in red.

Table A.3. Model performance statistics for east and north components of velocity at the northern ADCP location at Noster (ID347) for June – September 2020.

	ADCP Depth (bin)	Model Depth	Metric	East	North
Surface	19.3 m (24)	21.4	d_2	0.64	0.81
			MAE	0.02	0.05
			RMSE	0.02	0.06
Middle	35.3 m (16)	33.6	d_2	0.57	0.82
			MAE	0.02	0.05
			RMSE	0.03	0.07
Bottom	65.3 m (1)	58.1	d_2	0.71	0.85
			MAE	0.02	0.04
			RMSE	0.03	0.06

Figure A.4. Scatter plot of observed and modelled velocity at three depths at the Noster ADCP location (ID347) from June – September 2020. Observed data are in blue, model results in red.

A.3.2 June – September 2020, Seaforth (ID348)

Results of the model comparison with data from the Seaforth site (ID348) are presented in Figures A.5 – A.7 and Table A.4.

Model skill scores, MAE and RMSE values for the sea surface height were 0.99, 0.14 and 0.17 respectively (Figure A.5, Table A.2). North and east components of velocity at the ADCP location were well reproduced by the model, with values of the model skill, d_2, of about 0.8 for both components (Figure A.6, Table A.4). The scatter plots shown in Figure A.7 demonstrate that the modelled currents were broadly of the same magnitude and direction as the observed data.
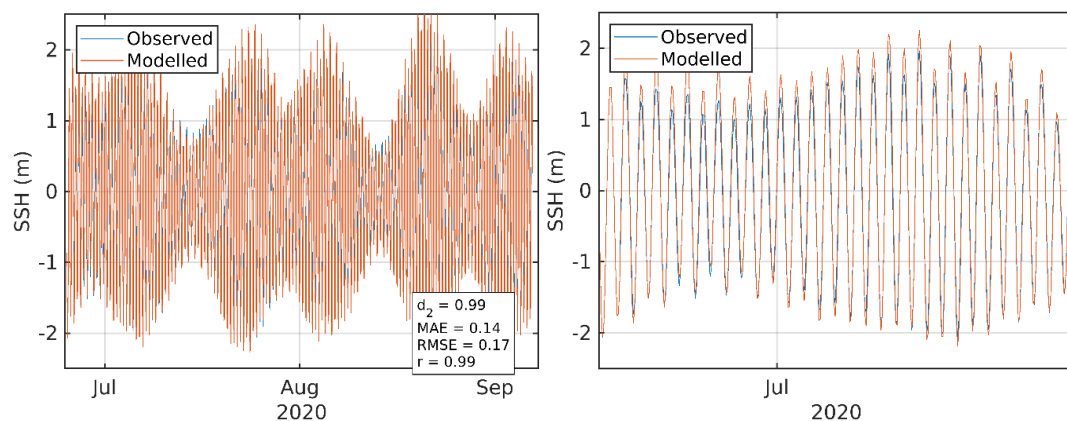
Figure A.5. Comparison between observed (blue) and modelled (red) sea surface height from June – September 2020 at the Seaforth ADCP location (ID348) using model parameter values from Table A. Both the full record (left) and a subset of 15 days (right) are shown.
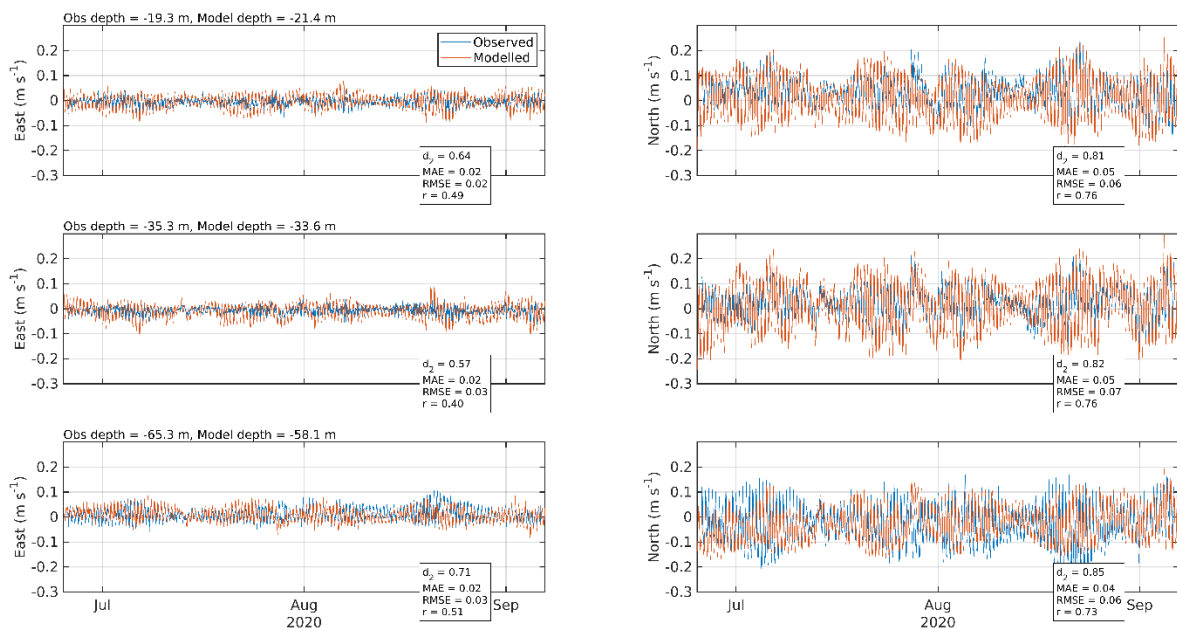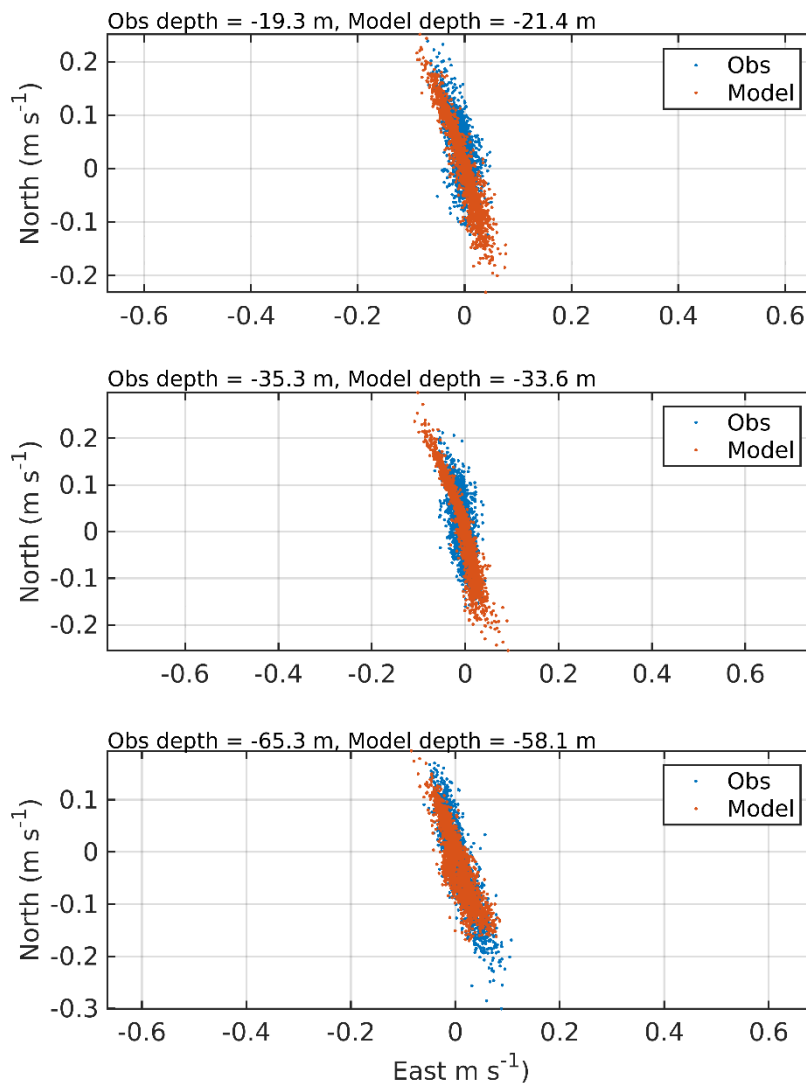
.
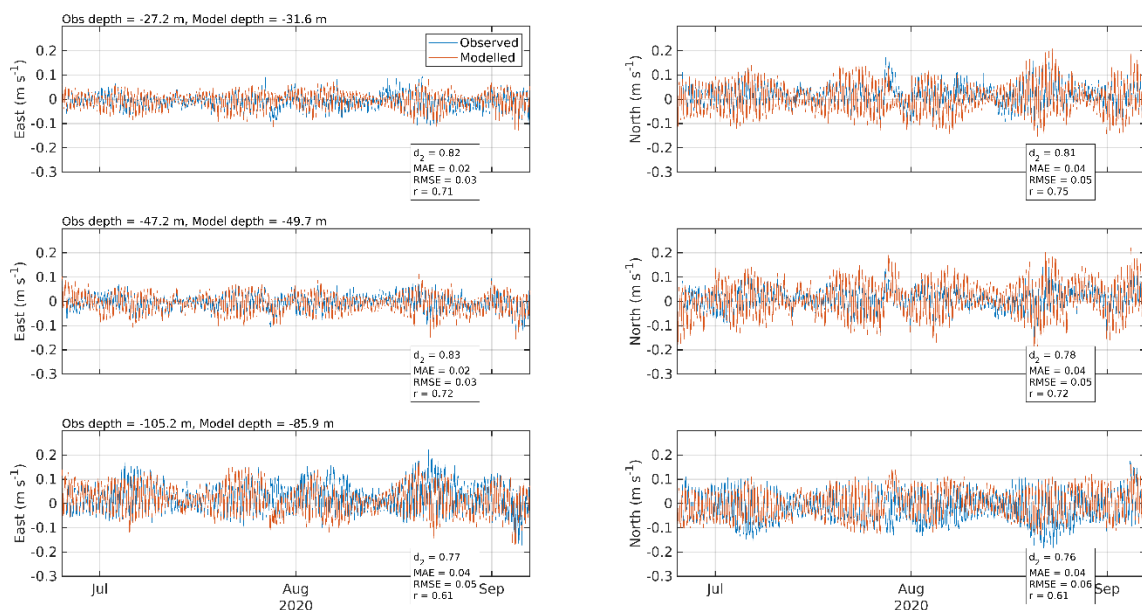
Figure A.6. Comparison between observed and modelled East (top) and North (bottom) components of velocity at three depths at the Seaforth ADCP location (ID348) for June – September 2020. Observed data are in blue, model results in red.

Table A.4. Model performance statistics for east and north components of velocity at the southern ADCP location at Seaforth (ID348) for June – September 2020.

	ADCP Depth (bin)	Model Depth	Metric	East	North
Surface	27.2 m (40)	31.6	d_2	0.82	0.81
			MAE	0.02	0.04
			RMSE	0.03	0.05
Middle	47.2 m (30)	49.7	d_2	0.83	0.78
			MAE	0.02	0.04
			RMSE	0.03	0.05
Bottom	105.2 m (1)	85.9	d_2	0.77	0.76
			MAE	0.04	0.04
			RMSE	0.05	0.06
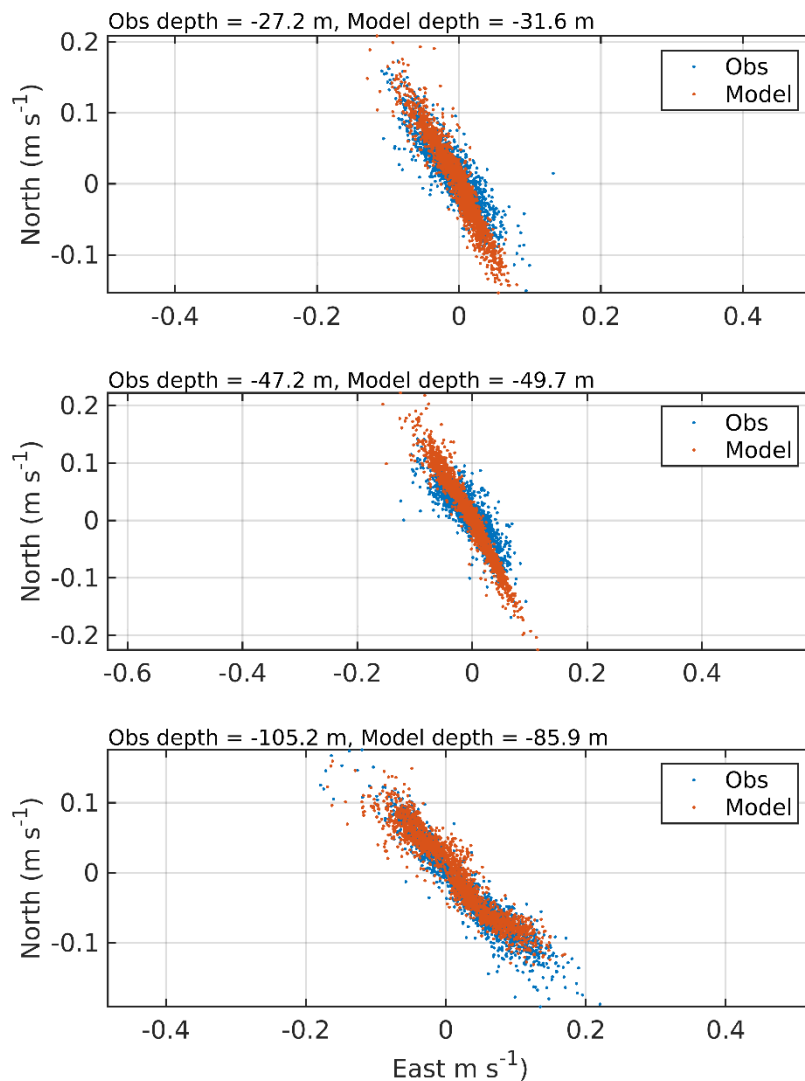
Figure A.7. Scatter plot of observed (blue) and modelled 9red) velocity at three depths at the Seaforth ADCP location (ID348) from June – September 2020.

A.4　Modelled Flow Fields, February – March 2018

Model simulations were also performed for February – March 2018, when dye release studies were undertaken in Loch Seaforth. The model was configured exactly as described above, with the spin-up and main runs covering the periods:

1. Spin-up:　　20th February – 25th February 2018
2. Main Run:　25th February – 29th March 2018

Modelled sea surface height for the main run is shown in Figure A.8. The simulation period covered a large spring tide and small neap tide. These periods were used for the dispersion modelling. The dye releases took place on 25th and 28th February, with the seven release times indicated by the vertical dashed lines.
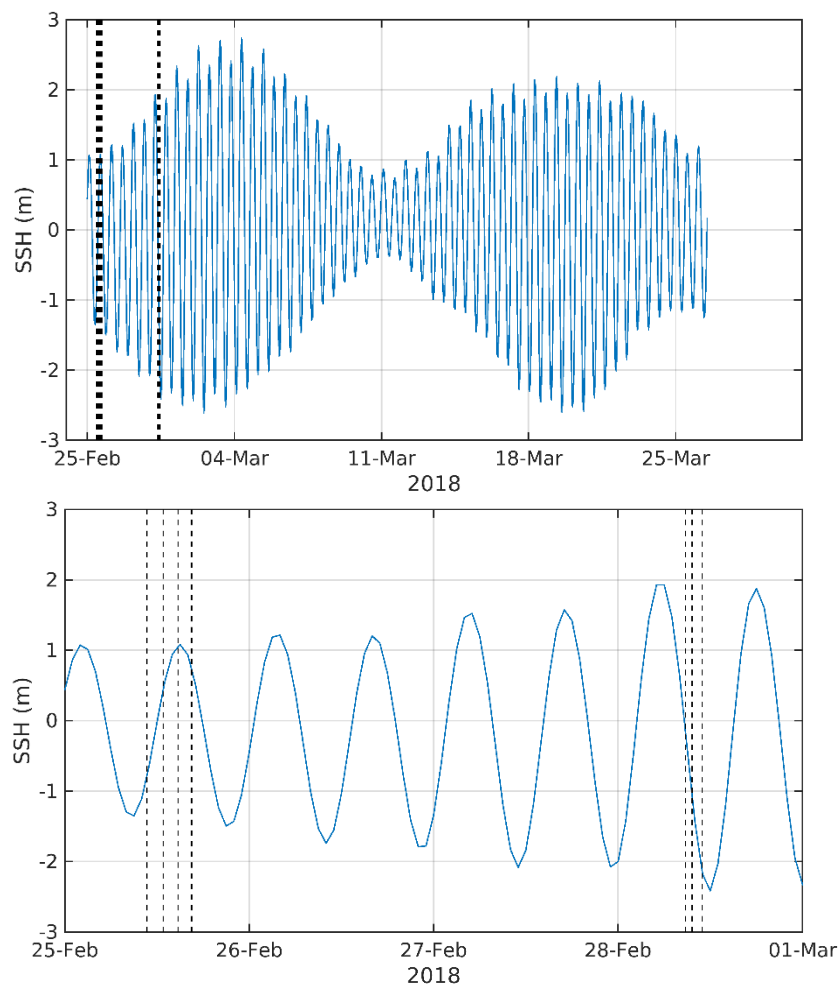
Figure A.8. Modelled sea surface height (SSH) at the Seaforth farm during February – March 2018 (top). The times of the dye releases are indicated by the vertical dashed lines. The period 25th – 28th February 2018, when the dye releases took place, is highlighted (bottom).

Although ADCPs were not deployed during this period, time series of velocity at the ID347 and ID348 locations are plotted in Figures A.9 and A.10 respectively. Time series were plotted for model layers 1, 5 and 10, corresponding to near-surface, mid-depth and near-bed depths. The modelled velocity are plotted as scatter plots in Figure A.11, for comparison with Figures A.4 and A.7.

Modelled surface layer velocity vectors corresponding to the seventh dye release on 28th February are mapped in Figure A.12.
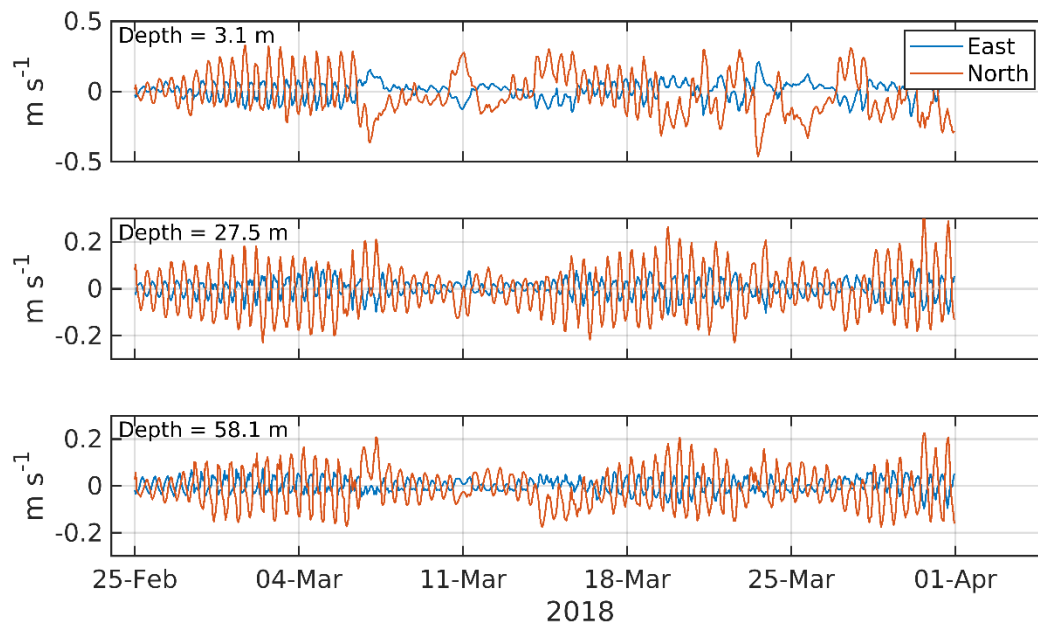
Figure A.9. Modelled East (blue) and North (red) components of velocity for three depths (3.1m, 27.5, and 58.1m) at the location of ADCP deployment ID347 but for the period February – March 2018.
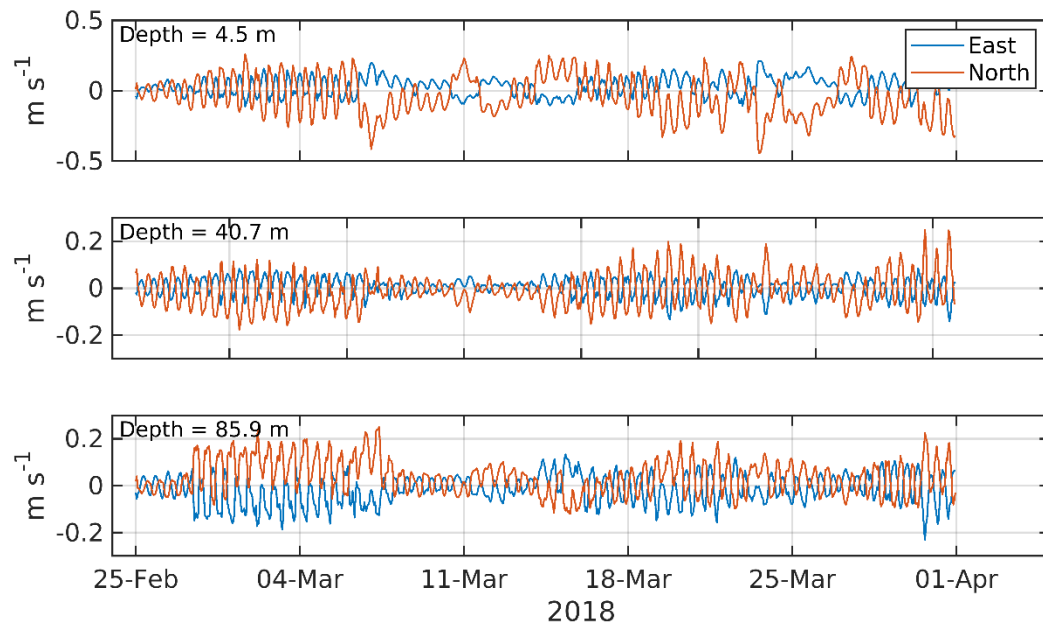
Figure A.10. Modelled East (blue) and North (red) components of velocity for three depths (4.5m, 40.7, and 85.9m) at the location of ADCP deployment ID348 but for the period February – March 2018.
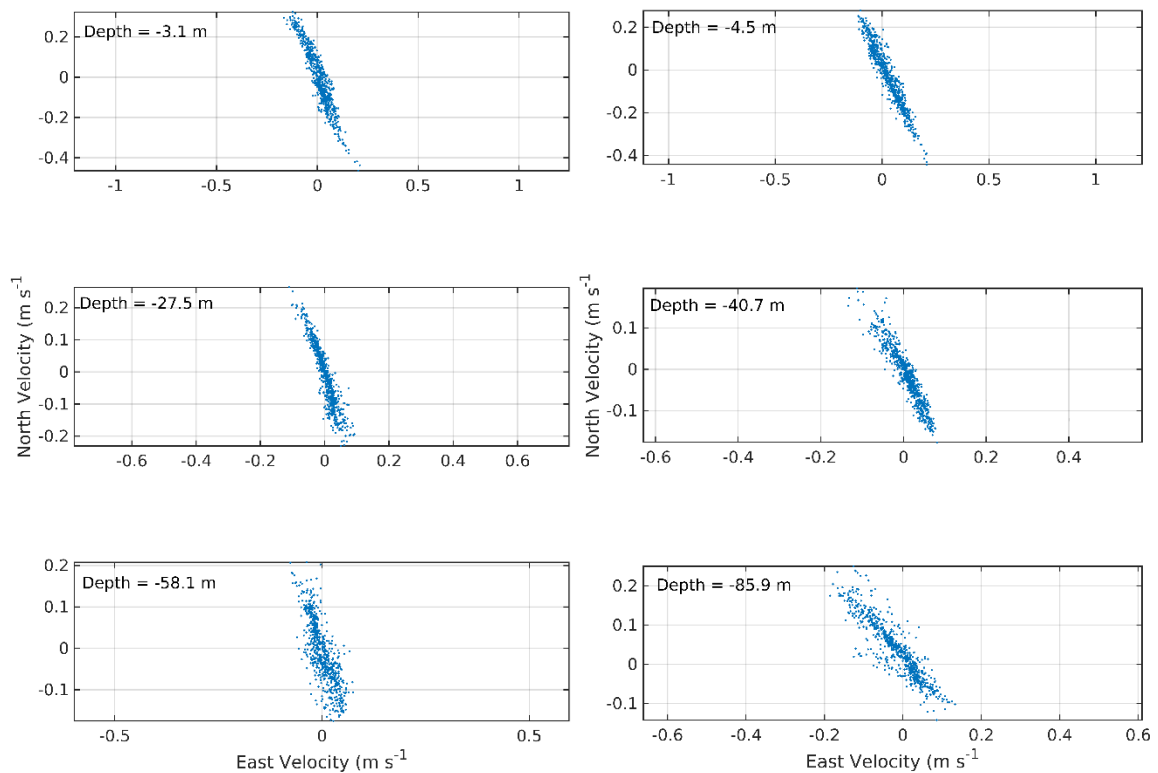
Figure A.11. Scatter plots of modelled velocities from ADCP deployment locations ID347 at Noster (left) and ID348 at Seaforth (right) from model layers 1 (top), 5 (middle) and 10 (bottom). The depths of each layer at each location are indicated.
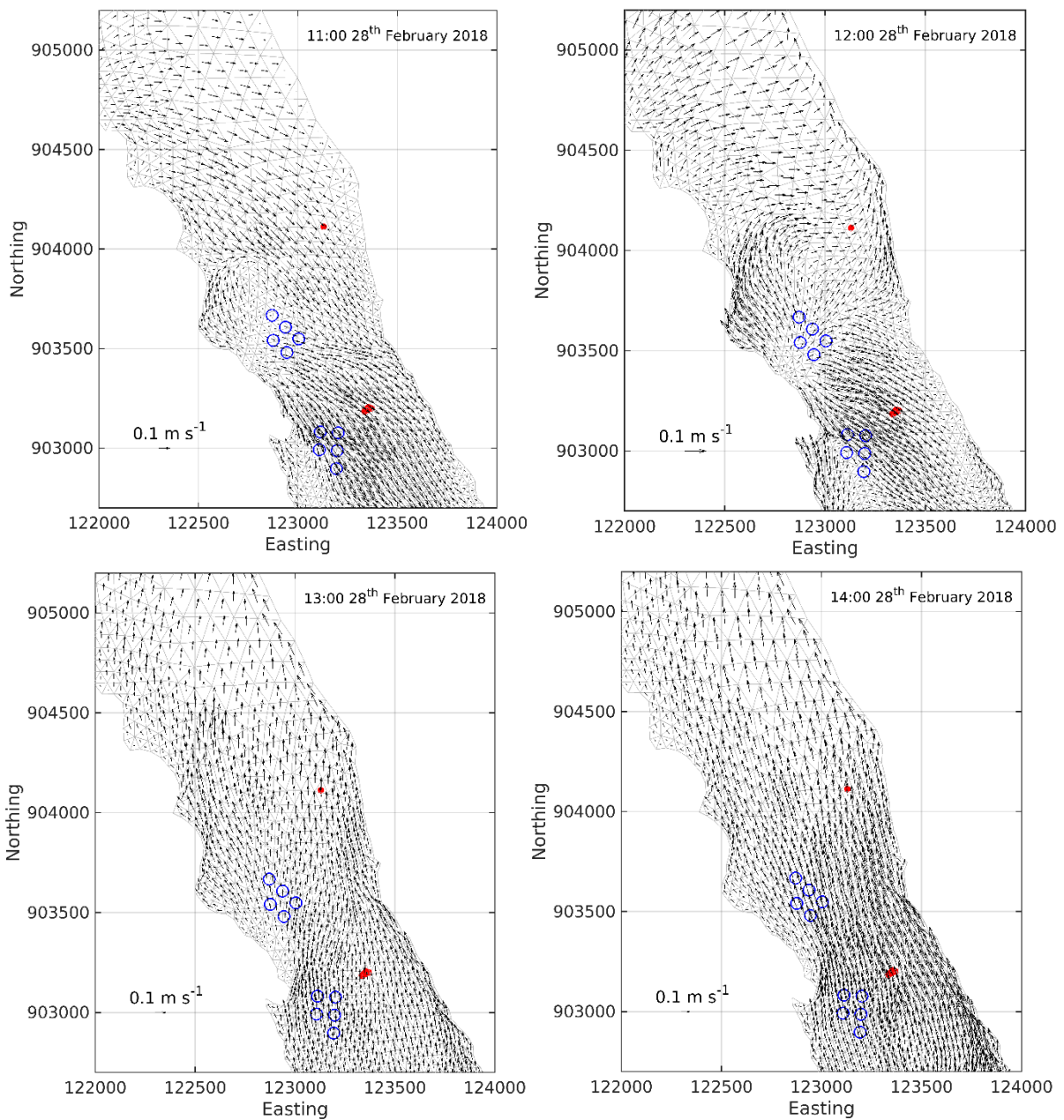
Figure A.12. Modelled surface layer vectors in Loch Seaforth during dye release number 7 at 11:00 28th February 2018 (top left), 12:00 28th February 2018 (top right), 13:00 28th February 2018 (bottom left) and 14:00 28th February 2018 (bottom right). The dye release locations (●) and farm pens (○) are marked.

A.5   References

Burchard, H., 2002. Applied turbulence modeling in marine waters. Springer:Berlin-Heidelberg-New York-Barcelona-Hong Kong-London-Milan Paris-Tokyo, 215pp.

Chen, C., H. Liu, and R.C. Beardsley, 2003. An unstructured, finite-volume, three-dimensional, primitive equation ocean model: Application to coastal ocean and estuaries. J. Atmos. Ocean. Tech., 20, 159 – 186.

Gillibrand, P.A., Walters, R.A., and McIlvenny, J., 2016. Numerical simulations of the effects of a tidal turbine array on near-bed velocity and local bed shear stress. *Energies*, vol 9, no. 10, pp. 852. DOI: 10.3390/en9100852

Walters, R.A.; Gillibrand, P.A.; Bell, R.; Lane, E.M. 2010. A Study of Tides and Currents in Cook Strait, New Zealand. Ocean Dyn., 60, 1559-1580.

Willmott, C. J.; Ackleson, S. G.; Davis, R. E.; Feddema, J. J.; Klink, K. M.; Legates, D. R. O'Donnell, J.; Rowe, C. M. 1985. Statistics for evaluation and comparison of models, J. Geophys. Res., 90, 8995– 9005.

ANNEX B. DISPERSION MODEL DESCRIPTION

B.1 "unptrack" Model Description

Modelling of bath treatments will be undertaken using a bespoke particle tracking model (Gillibrand, 2021), forced by the flow fields from the hydrodynamic model described above, to simulate the discharges and subsequent dispersion of veterinary medicines.

The dispersion model has been developed from an earlier particle-tracking model code that has been used to simulate the transport and dispersal of pelagic organisms, including sea lice larvae (Gillibrand and Willis, 2007) and harmful algal blooms (Gillibrand et al., 2016), and solute veterinary medicines (Willis et al., 2005) in Scottish coastal waters. The new model, unptrack (Gillibrand, 2021), has been developed to use flow data from unstructured mesh hydrodynamic models. The model approach for a veterinary medicine is the same as for live organisms except that the medicine has no biological behaviour but instead undergoes chemical decay; the numerical particles in the model represent "droplets" of medicine of known mass, which reduces over time at a rate determined by a specified half-life. Particles are released at pen locations at specified times, according to a treatment schedule. The number of particles combined with their initial mass represents the mass of medicine required to treat a pen. The particles are then subject to advection, from the modelled flow fields, and horizontal and vertical diffusion. Particle locations are tracked throughout the simulation and output to file every hour, together with particle properties such as particle age and the mass of medicine represented (subject to decay). From the particle locations, concentrations of medicine are calculated and compliance with Environmental Quality Standards (EQS) can be assessed where appropriate.

Velocity data to drive the model can be obtained from current meter (ADCP) observations or from hydrodynamic model simulations. In the case of the latter, the particle-tracking model will use the same numerical grid as the hydrodynamic model, with the modelled velocity fields used to advect the numerical particles. In the case of the former, a numerical grid is constructed to cover the area of the simulated dispersion, and the observed current data applied at each of the grid nodes; in this case, the velocity field experienced by the numerical particles is spatially non-varying in the horizontal, although vertical shear can be present if multiple current meters, or multiple bins from an ADCP deployment, are used. In both cases, realistic bathymetry can be used, although this is not expected to be a critical factor in the dispersion of bath treatments.

B.2 Mathematical Framework

Within the particle tracking model, particles are advected by the velocity field and mixed by horizontal and vertical eddy diffusion, simulating the physical transport and dispersion of the cells. The mathematical framework of the model follows standard methodology for advection and diffusion of particles (e.g. Allen, 1982; Hunter et al., 1993; Ross and Sharples, 2004; Visser, 1997), whereby the location $X^{t+\Delta t}_P = X^{t+\Delta t}_P(x,y,z)$ of particle P at time $t+\Delta t$, can be expressed as:

$$X_P^{t+\Delta t} = X_P^t + \Delta t\left[\vec{U}_P + w_P\right] + \delta_H + \delta_Z \qquad (1)$$

where $\vec{U}_P$(x,y,z) is the 3D model velocity vector at the particle location, w_p is an additional vertical motion term due to, for example, particle settling or vertical migration and Δt is the model time step. Particle advection is treated using a fourth-order Runge-Kutta algorithm. Horizontal and vertical eddy diffusion are represented in the model by the "random walk" displacements δ_H and δ_Z respectively, given by (Proctor et al., 1994):

$$\delta_H = R[6.K_H.\Delta t]^{1/2}$$

$$\delta_Z = R[6.K_V.\Delta t]^{1/2}$$

(2)

where R is a real random number uniformly distributed over the range -1 ≤ R ≤ 1, and K_H and K_V are the horizontal and vertical eddy diffusivities respectively. Typically, a small constant eddy diffusivity is used e.g. $K_H = 0.1$ m^2 s^{-1}. The choice of eddy diffusivity can be informed by dye release experiments where available.

A choice of vertical diffusion coefficient must also be made, and the knowledge base here is less certain. A value of $K_V = 0.001$ m^{2}s^{-1} is thought to be reasonably conservative for near-surface waters on the UK continental shelf.

In Equation (1) for solute substances, w_p represents additional vertical motion of the particle due to, for example, buoyancy. For the present simulations, $w_p = 0$ since the bath treatments simulated here are administered in the pens with the medicine mixed into ambient seawater. Chemical decay is simulated by varying the particle properties. At the time of release, each numerical particle represents a mass, M_0, of the dissolved substance. The age since release, t_p, of every particle is stored, and the chemical mass, M_P, represented by each particle changes according to:

$$M_P = M_0 e^{\gamma t_p}$$

(3)

where $\gamma = \ln(0.5)/T_D$ and T_D is the half-life of the chemical decay. The mass M_P of every particle is stored in each output file.

B.3   Model Tests

The dispersion model has been subjected to various tests, including the standard Brickman test (Brickman et al., 2009) to ensure advection is treated accurately in spatially-varying flow fields (Figure 9.). The model was tested using a range of time steps from 36s to 3600s and successfully reproduced the final particle location distribution for all time steps (Figure). In the simulations described below, a time step of 600s was used.
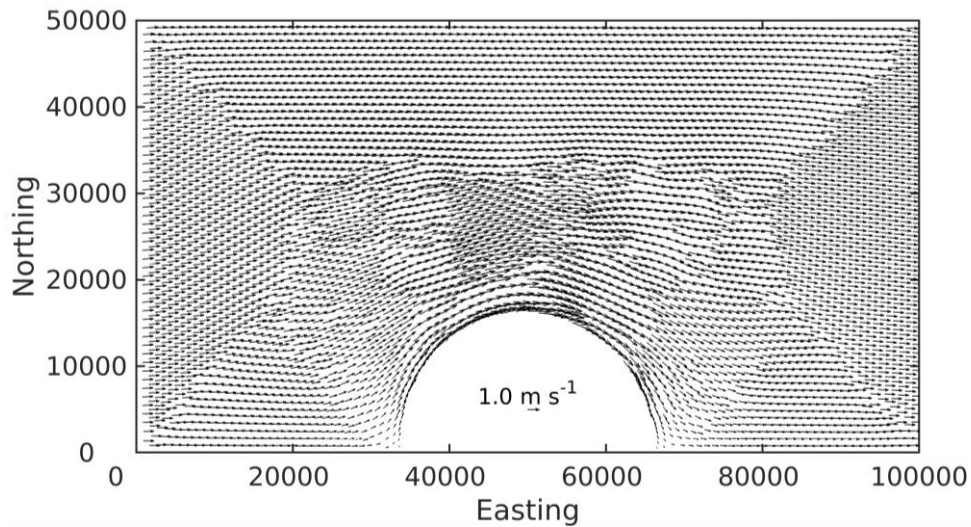
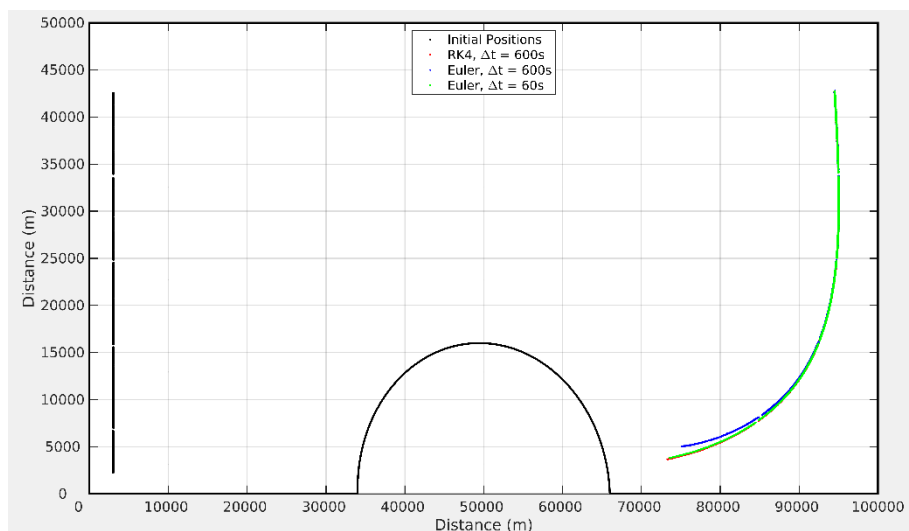*Figure B.1. Flow vectors for the Brickman test. Flow at the left-hand boundary is 1 m s⁻¹.*

Figure B.2. Results from the advection test. Particle locations 24 hours after release from the source locations at x = 3000m are shown to be independent of time step for 36 ≤ Δt ≤ 3600s, and in the correct distribution (Brickman et al., 2009).

The model was also tested for diffusion and chemical decay. The random walk algorithm correctly simulated the increase in variance in the particle locations with specified horizontal dispersion coefficients of 0.1 m^2s^{-1} and 1.0 m^2s^{-1}. A fundamental property of a lagrangian particle tracking model is that it maintains an initially uniform distribution of particles uniform for all time. This is known as the well-mixed condition (Brickman and Smith, 2002; North et al., 2006). This test was successfully replicated by unptrack (Gillibrand, 2021). Chemical decay was similarly tested and the modelled concentration decayed with the specified half-life. These tests are not reported further here but details can be found in Gillibrand (2021).

B.4 Model Evaluation against Dye Track Data

Dye releases took place on 25th and 28th February 2018. The times and locations of the releases are detailed in Table . Note that the seventh release, which was tracked for more than three hours, was released further north than previous releases (Figure A.1). For each release, 0.5 kg of dye was discharged.

Table B.1. Details of the dye releases undertaken in February 2018.

Release	Date	Time	Easting	Northing
1	25/02/2018	10:40	123354	903206
2	25/02/2018	12:49	123345	903196
3	25/02/2018	14:44	123369	903201
4	25/02/2018	16:29	123335	903185
5	28/02/2018	08:45	123355	903194
6	28/02/2018	09:36	123347	903192
7	28/02/2018	10:58	123129	904113

Following release, multiple discrete surveys of the dye patch were undertaken. From these data, the location of the centre of the dye patch was estimated over time.

The modelling simulated these releases by releasing particles in discrete patches at the times given in Table B.1. Modelled particle locations were recorded every 10 minutes, and the mean particle location (assumed to represent the centre of the patch) was calculated. Particles were released in a 1m radius circle about the release location over a depth range of 0 – 2 m. The tracks of the modelled particle patch centres were then compared to the observed data tracks.

The simulated dye patches during the Release 7 (the longest tracked release) are shown in Figure B.3. At 11:00 on 28th February, immediately following Release 7 to the north-east of the Noster site, the small patch of Release 7 is evident. The merged patch from the earlier releases 5 and 6 is still evident to the south (Release 7 took place further north to avoid contamination from these earlier releases). An hour later, at 12:00 on 28th, Release 7 has moved eastwards towards the shoreline. In the following hours, the patch tracks northwards following the shoreline.

The observed and modelled dye tracks from the releases on 25th February are shown in Figure B.4 and those from 28th February in Figure B.5. The model captures the observed pathways of the releases that were tracked for longer (numbers 1, 2, 7) well.

The success in reproducing the transport pathways of the dye releases suggests that the surface flow fields from the February – March 2018 FVCOM simulation are a realistic representation of the flows.
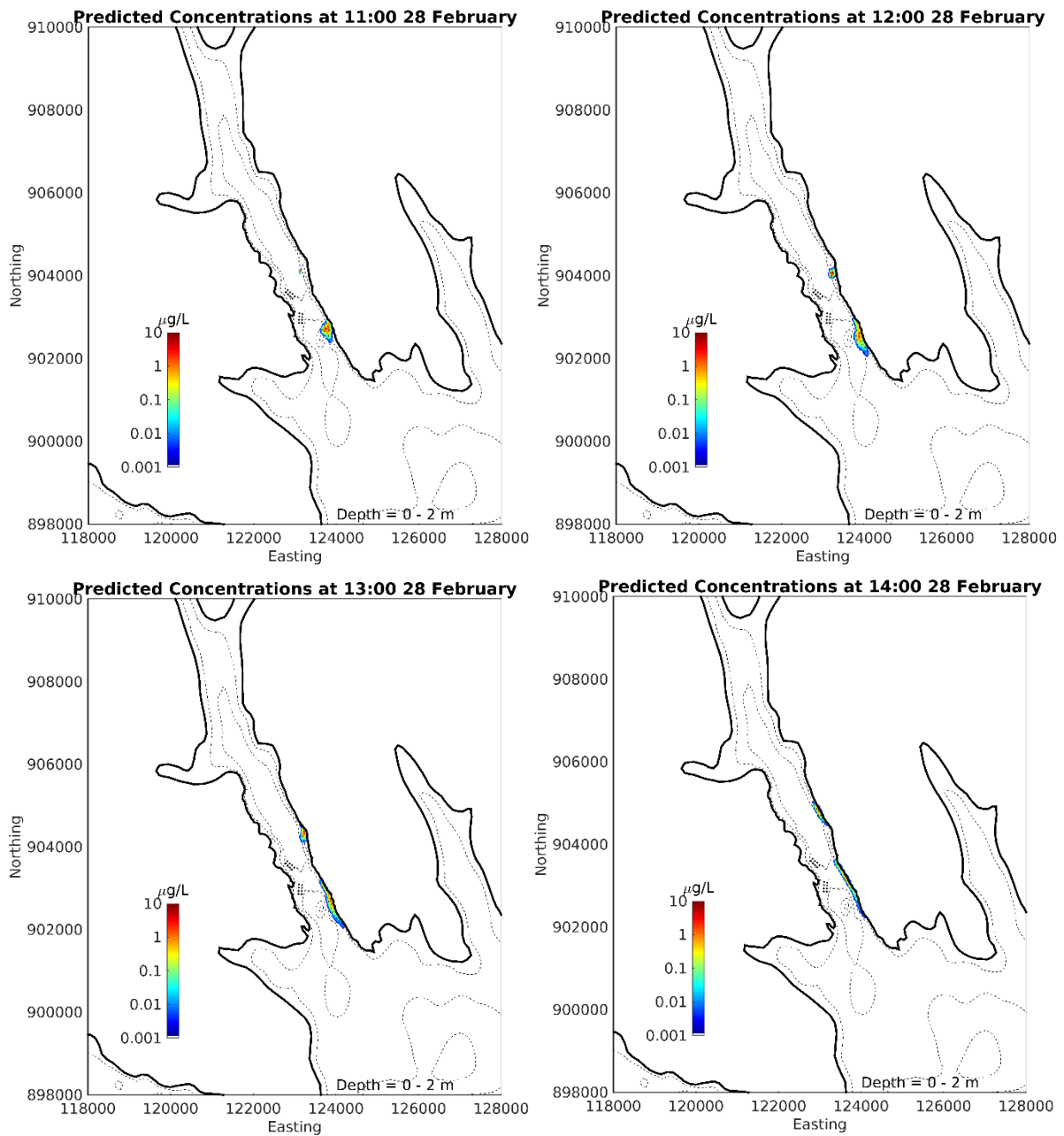
Figure B.3. Simulated dye concentrations (µg/L) on 28th February 2018, following Releases 5, 6 and 7 (Table B.1). Pen locations at the Seaforth and Noster sites are indicated (•).
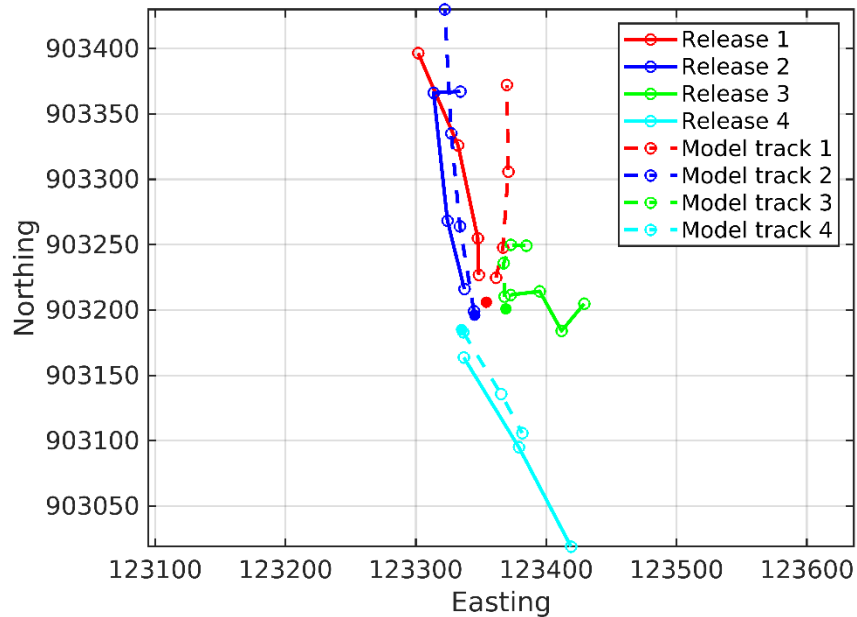
Figure B.4. Observed (solid lines) and modelled (dashed lines) dye tracks from four releases (nos. 1 – 4) on 25th February 2018. The filled circles mark the release location of each release, with the open circles marking the patch centre for each subsequent survey.
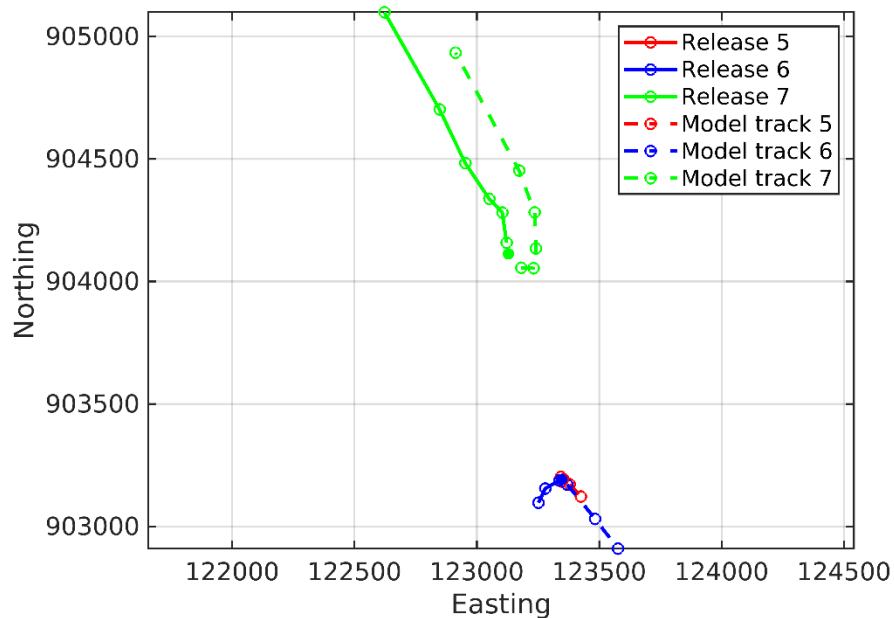

Figure B.5. Observed (solid lines) and modelled (dashed lines) dye tracks from three releases (nos. 5 – 7) on 28th February 2018.

B.5 References

Allen, C.M., 1982. Numerical simulation of contaminant dispersion in estuary flows. Proc. Royal. Soc. London (A), 381, 179–194.

Brickman, D., Ådlandsvik, B., Thygesen, U.H., Parada, C., Rose, K., Hermann, A.J. and Edwards, K., 2009. Particle Tracking. In: Manual of Recommended Practices for Modelling Physical – Biological Interactions during Fish Early Life, pp. 27 – 42. Ed. by E. W. North, A. Gallego, and P. Petitgas. ICES Cooperative Research Report No. 295. 111 pp.

Brickman, D., and P.C. Smith Lagrangian stochastic modeling in coastal oceanography. J. Atmos. Ocean Tech., 19, 83-99, 2002.

Gillibrand, P.A., 2021. Unptrack User Guide. Mowi Scotland Ltd., February 2021, 31pp. https://github.com/gillibrandpa/unptrack

Gillibrand, P.A., B. Siemering, P.I. Miller and K. Davidson, 2016. Individual-Based Modelling of the Development and Transport of a Karenia mikimotoi Bloom on the North-West European Continental Shelf. Harmful Algae, DOI: 10.1016/j.hal.2015.11.011

Gillibrand, P.A. and K.J. Willis, 2007. Dispersal of Sea Lice Larvae from Salmon Farms: A Model Study of the Influence of Environmental Conditions and Larval Behaviour. Aquatic Biology, 1, 73-75.

Hunter J.R., Craig, P.D., Phillips, H.E., 1993. On the use of random walk models with spatially variable diffusivity. J Comput. Phys., 106:366–376

North, E.W., R.R. Hood, S.-Y. Chao and L.P. Sanford. Using a random displacement model to simulate turbulent particle motion in a baroclinic frontal zone: A new implementation scheme and model performance tests. J. Mar. Sys., 60, 365-380, 2006.

Proctor, R., R.A. Flather and A.J. Elliott, 1994. Modelling tides and surface drift in the Arabian Gulf---application to the Gulf oil spill. Continental Shelf Research, 14, 531-545.

Ross, O.N., Sharples, J., 2004. Recipe for 1-D Lagrangian particle tracking models in space-varying diffusivity. Limnology and Oceanography: Methods, 2, 289-302.

Visser, A.W., 1997. Using random walk models to simulate the vertical distribution of particles in a turbulent water column. Mar. Ecol. Prog. Ser., 158, 275-281.